Chapter 8

SEMICONDUCTOR IMAGE SENSING

N. Blanc[1], P. Giffard[3] ,P. Seitz [2], P. Buchschacher[1], V. Nguyen[3], M. Hoheisel[4],
[1]*CSEM SA, Photonics Division, Technoparkstrasse 1, CH-8005 Zurich, Switzerland*
[2]*CSEM SA, Research Center for Nanomedicine, Schulstr. 1, CH-7203 Landquart, Switzerland*
[3]*CEA-LETI Minatec, F-Grenoble, France*
[4]*Siemens AG, D-Forchheim, Germany*

Abstract: Silicon is an excellent detector material for electromagnetic radiation in the wavelength range of 0.1 to 1000 nm. In the visible spectral range (400-700 nm), external quantum efficiencies approaching 100% are obtained. When combined with the amazing miniaturization capabilities of the semiconductor industry, this fact explains why silicon is the material of choice for very efficient, highly integrated, cost-effective image sensors: In 2007 about one billion image sensors were produced and employed in camera systems. Profiting from the unrelenting progress of semiconductor technology, silicon-based image sensors with astounding performance have been demonstrated, in terms of resolution, pixel size, data rate, sensitivity, time resolution and functionality: 111 million pixels on a single CCD chip were produced, pixels with a period of 1.2 μm were fabricated, sustainable image acquisition and readout rates of 4 billion pixels per second were realized, single-photon sensitivity at room temperature and at video rates was achieved, timing resolution of the pixels in lock-in image sensors below 5 ps was obtained, and the processing complexity of "smart pixels" was raised to several ten transistor functions per pixel. The future of semiconductor image sensing lies in the extension of the accessible wavelength range to the infrared spectrum (1.5-10 μm), the development of affordable, high-performance X-ray image sensors in particular for the medical energy range (20-120 keV), the realization of sensitive and cost-effective sensors for Terahertz imaging (100-500 μm), as well as the integration of an increasing amount of analog and digital functionality on single-chip custom camera systems. The Holy Grail is the "seeing chip", capable of analyzing the contents of a scene and of recognizing individual objects of interest.

Key words: Solid-state image sensing. Electronic imaging. X-ray imaging. Infrared sensing. Seeing chips.

1 INTRODUCTION

Over the last decade, electronic imaging has made tremendous progresses, basically replacing film-based cameras in almost all application fields, including consumer, security, industrial and scientific applications. These cameras rely on the excellent optoelectronic properties of semiconductor materials, with silicon being in most cases the material of choice. High quantum efficiency over the visible range and the cost effective manufacturing capability of the semiconductor industry have enabled the production of image sensors at affordable prices with excellent performances, in particular in terms of spatial resolution, pixel size, dynamic range and sensitivity. Until the year 2000 the large majority of commercially available electronics cameras and camcorders were based on CCDs (Charge Coupled Devices). Today CCDs still play an important role in electronic imaging, due to their high performances providing for example spatial resolution of up to 111M pixels, dynamic range in excess of 80dB and sensitivity down to single-photon detection. However, Complementary Metal-Oxide-Semiconductor (CMOS) image sensors have been since the 1990's the subject of significant development. They take advantage of the capability to integrate analog and digital circuits on chip for the control and readout electronics. This on one hand enables the manufacture of cost-effective image sensors and on the other hand allows the realization of imagers with added functionalities, leading to increasingly smarter and more compact imaging devices. As a result, CMOS image sensors have today become worldwide the dominating technology both in terms of units sold as well as in terms of revenues. CMOS image sensors are now widely used for consumer applications, such as in compact digital still picture cameras (DSCs), mobile phones and camcorders, as well as in numerous other fields, including surveillance, security, robotics, automotive, industrial control and even medical applications.

CMOS image sensors clearly profit from the progresses realized in the semiconductor industry and the continuous trend towards miniaturization, smaller minimal feature size and the increased numbers of transistors/pixels per unit area, following in this regards Moore's law as often referred to for other integrated circuits such as processors and memories. On the other hand the trend in the development of image sensors goes beyond just a race for more pixels and a higher level of integration. Image sensors are more and more used for applications covering a significant broader spectral range, from X-ray up to Terahertz imaging. Moreover the development of smart imagers opens up completely new possibilities, for example in three-

dimensional imaging, object tracking, smart intrusion detection or spectral imaging.

The present chapter gives an overview on fundamentals of semiconductor image sensing and technology, giving insights in current technological trends and the state-of-the art in high-sensitivity electronic imaging. This is followed by application examples in high-speed imaging, color imaging and optical 3D Time-Of-Flight imaging. While many applications and products are focused on the visible range of the electromagnetic spectrum, the extension towards shorter wavelength (e.g. X-ray imaging) and longer wavelength (such as infrared and Terahertz imaging) is gaining in importance. Examples of IR sensors include Quantum Well IR photodetectors, bolometers and HgCdTe sensors. Magnetic resonance and ultrasound imaging in turn are not addressed within the scope of this chapter.

2 FUNDAMENTALS OF SEMICONDUCTOR IMAGE SENSING

2.1 Interaction of light and semiconductor

The capability of solid-state image sensors to detect light is related to their semiconducting properties. The interaction of light and semiconductors has two principal components. First light waves travel at a reduced speed $c_{mat} = c_{vac}/n$ where n is the refractive index of the material and $c_{vac} = 3\times10^8$ m/s is the speed of light in vacuum. Secondly the incident light intensity I_0 (W/m^2) is absorbed exponentially with the thickness x of material through which it travelled, according to Beer's law:

$$I(x) = I_0\, e^{-\alpha x} \qquad \textbf{(1)}$$

The absorption coefficient α (in units of cm^{-1}) depends strongly on the wavelength and thus the energy of the incident light: For energies below the bandgap E_g, the material is essentially transparent. For energies larger than the bandgap, the material absorbs the incident radiation. The higher the energy (the lower the wavelength), the smaller is the penetration depth. For direct-bandgap semiconductor materials such as GaAs the $\alpha(E)$ curve is even steeper than for indirect-bandgap materials such as silicon (figure 1). The bandgap of the material used has thus a direct impact on the spectral range that can be addressed. Silicon with a bandgap of E_g=1.1eV at room temperature has a cut-off frequency of 1.1µm, whereas Germanium with a

lower bandgap of 0.67eV leads to a cut-off frequency of 1.8μm enabling to address applications in the near infrared part of the spectrum.

$$\lambda_c(\mu m) = \frac{1.24}{E_g(eV)} \qquad (2)$$

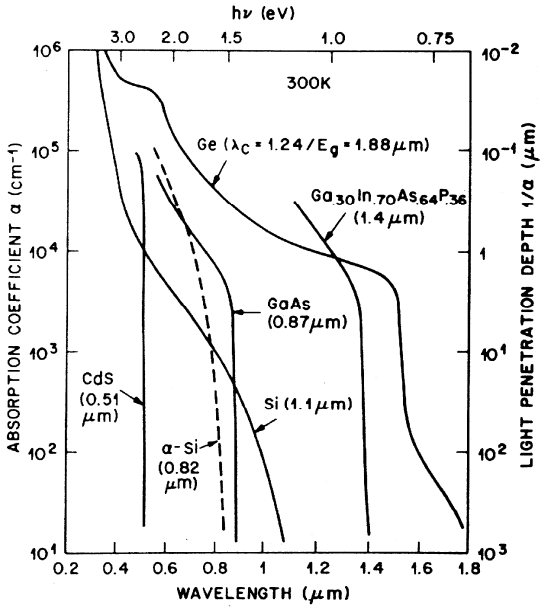

Figure 1. Optical absorption coefficients and light penetration depths for various semiconductor materials [1].

2.2 Quantum Efficiency

The processes of photon absorption and thermalization of charge pairs happen in sequence, contrary to the generation of light via a recombination process, requiring the simultaneous presence of a suitable phonon in indirect-bandgap materials to satisfy momentum conservation. For this reason, all semiconductor materials are excellent photodetectors, independent of their type of bandgap, direct or indirect. Virtually 100% of the incident photons with energy above the bandgap could therefore be detected, in principle. In actual devices, the external quantum efficiency (QE), defined as η = number of photogenerated charge pairs / number of incident photons, is smaller than 100% for the following reasons:

(1) Fresnel reflection of the incident light at the surface of the device
(2) Multiple reflections in thin layers covering the device. This causes the characteristic thin film interference oscillations in the spectrum.
(3) Absorption of the incident light either in the covering layers or in the electrically inactive part of the semiconductor near the surface.
(4) Absorption deep in the semiconductor, at a distance greater than the diffusion length L, where charge carrier pairs recombine instead of being able to diffuse to the depletion region of the photodetector near the surface.
(5) The semiconductor is too thin (too transparent) so that not all the incident light is absorbed and parts of it (the longer wavelengths) are transmitted.

Figure 2 shows the measured spectral QE of an n^- p-substrate silicon photodiode, realized in a 2 µm CMOS process (Orbit Inc., Sunnyvale, USA) that can be explained with a model taking into account the effects mentioned above [2].

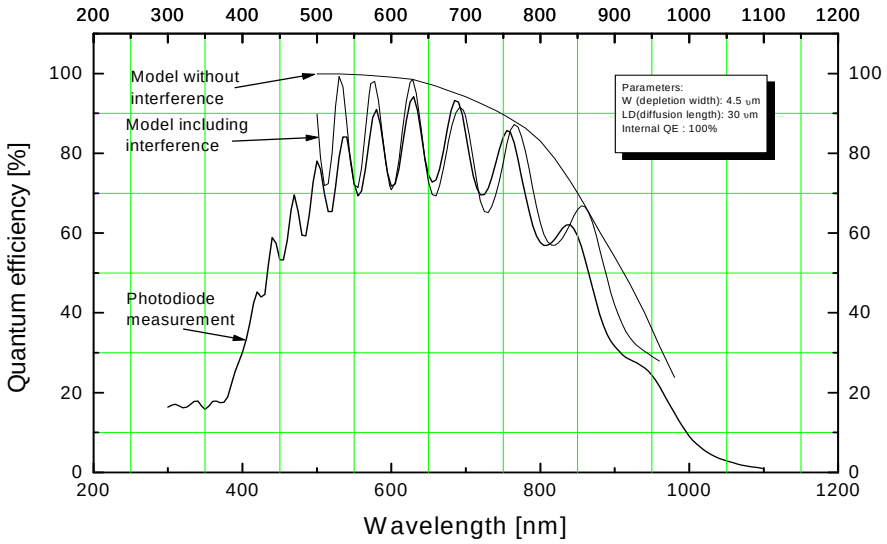

Figure 2. Comparison of a model of the quantum efficiency (dashed line) and actual measurements (solid line) of a photodiode, realized with a standard 2.0 µm CMOS process [2].

The QE η is a measure of the number of photogenerated electronic charge per incident photon. If, instead, the generated photocurrent I_{ph} [A] is

measured as a function of the incident light power P [W] at the wavelength λ, the corresponding responsivity R [in units of A/W] can be defined as

$$R = \frac{I_{ph}}{P} \qquad (3)$$

R is obviously related to the quantum efficiency η:

$$R(\lambda) = \frac{q\lambda}{hc}\eta(\lambda) \qquad (4)$$

with Planck's constant $h = 6.63\times10^{-34}$ Js, and the speed of light in vacuum $c = 3\times10^{8}$ m/s.

2.3 Temperature effects: dark current

The strongest impact of temperature is undoubtedly related to leakage currents. The so-called dark current (i.e. current measured without any applied optical signal) significantly varies from one technology to another with CCD still providing the best figures (below 1 pA/cm^2). Optimized CMOS processes for Image Sensing technologies report figures of a few 10s of pA (30pA/cm^2 - 50pA/cm^2) at room temperature. It is important to note that the dark current depends strongly on temperature, rendering high temperature applications very challenging. This dependence is essentially given by that of the intrinsic carrier concentration n_i in the semiconductor:

$$n_i \propto T^{\frac{3}{2}} e^{-\frac{E_g}{2kT}} \qquad (5)$$

With E_g = 1.11eV for silicon at room temperature the dark current is found to double roughly every 10 degrees. Experimentally this doubling occurs even every 7-8 degrees. Thus cooling the sensor by 25 degrees leads to a decrease of the dark current by almost a decade, which is significant and explain why most scientific cameras targeting applications with long exposure time (e.g. in astronomy) still need to be cooled. The current trend towards higher integration and smaller design features lead to typically higher doping levels and increased leakage current and dark current densities. This renders the realization of imagers providing high performances especially under low-light conditions even more challenging. In this specific case the higher integration / continuous trend towards

miniaturization basically works against key performance figures of imaging devices.

2.4 Photosensor principles: Photodiode and CCD

In image sensors the photo-generation of an electrical signal takes place in most cases either in a photodiode (i.e. a pn-junction) or in a MOS capacitance. Other approaches involve the use of specialized devices such as avalanche photodiodes and phototransistors. Generally speaking photodiodes are used in CMOS image sensors, whereas MOS capacitances are preferably implemented in CCD imagers. However Interline Transfer CCDs as mostly used in consumer cameras are typically based on photodiodes as photosensitive elements, whereas some CMOS imagers take advantage of photogates, a structure that is basically derived from CCD imagers.

Assuming a pixel size of $10\text{x}10\mu\text{m}^2$, a fill-factor of 100% and a quantum efficiency of 100%, an illumination level of 1 lux (which corresponds to about 10^{16} photons/s m^2 for white light) leads to a photocurrent of the order of 160fA. In order to effectively read-out such low signals special care must be taken. Different detection circuits have been developed over the last decades to address this challenge, the simplest and also most often implemented one being a source follower. In this approach the photo-generated current is first integrated during a given integration time T_{int} onto a capacitor C. After this integration/exposure time, the charge ΔQ accumulated is converted to an output voltage ΔV_{out} according to

$$\Delta \text{Q} = \int_{o}^{T_{\text{int}}} \text{i}_{\text{photo}}(t) \cdot dt \qquad (\mathbf{6})$$

$$\Delta \text{V}_{\text{out}} = (\Delta \text{Q} / C) \cdot g_a \qquad (\mathbf{7})$$

with $g_a \approx 0.6 - 0.8 \approx 1$ the “gain” of the source follower.

For a capacitance of $\text{C} = 10\,\text{fF}$, the conversion gain amounts to $\text{q/C} = 16\mu\text{V/e}$ leading to a measurable signal for typical charge packet of a few thousands of electrons. Higher conversion gain can be achieved by lowering the capacitance, or using current amplifier with very small feedback capacitances. This becomes mandatory if one wants to detect small signals, ultimately reaching for single electron and photon detection

3 SEMICONDUCTOR TECHNOLOGY FOR IMAGING

3.1 Silicon sensors

The unrelenting progress of semiconductor technology made it possible in the early 1960s to fabricate reliably several ten thousand transistors on the same chip. This capability was quickly used for the production of semiconductor image sensors using the then-available MOS process technology. These image sensors were based on the photodiode pixel architecture illustrated in Figure 3. Each pixel consists of a photodiode that can be connected individually to an output amplifier through a row-select transistor connecting the photodiode to a column electrode, and through a column-select transistor connecting the column to the video output line. The charge detector measures the stored photocharge on the reverse biased photodiode's depletion capacitance, and at the same time it performs a reset operation on the photodiode. These long signal lines result in effective capacitances at the input of the charge detector circuit of several pF, causing significant readout noise, typically in excess of 1000 electrons.

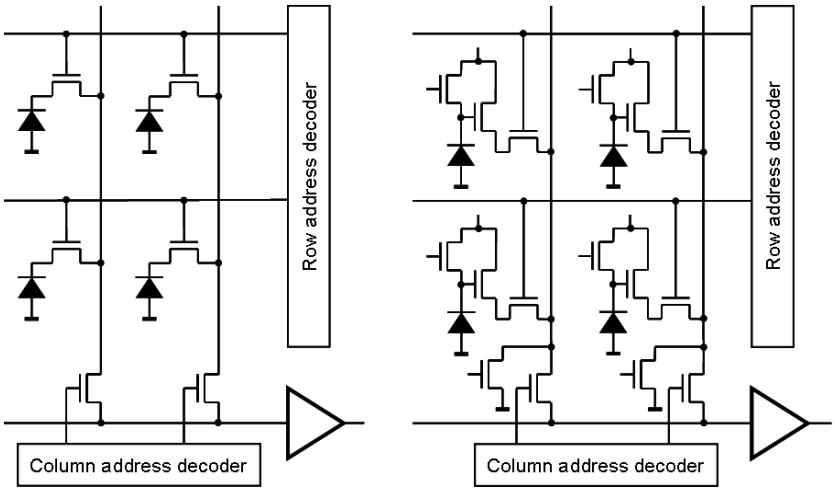

Figure 3. Architecture of photodiode based image sensors. (a) MOS or photodiode array, (b) CMOS compatible Active Pixel Sensor (APS) imager.

It was realized as early as 1968 that the invention of the active pixel sensor (APS) principle makes it possible to utilize a standard MOS or CMOS process for the fabrication of image sensors offering a similar imaging performance as CCDs [3]. The basic idea, illustrated in Fig. 3,

consists of supplying each pixel with its own source follower transistor, thus reducing the effective capacitance at its gate to a few tens of fF or less. Since each pixel still requires a row-select transistor and a means of resetting the photodiode – implemented with a reset transistor – a CMOS pixel with three transistors, a so-called 3T APS pixel, results. Surprisingly enough, this insight was only picked up commercially fifteen years later, once the urge to co-integrate analog and digital functionality on the same image sensor chip became significant [4]. For almost a decade afterwards, industrial CMOS processes were employed for the fabrication of CMOS image sensors and single-chip cameras of growing complexity, increasing pixel number and rising imaging performance.

In the late 1990s it became clear that the roadmap of mainstream CMOS technology, in order to satisfy the device scaling according to Moore's law, foresees technological changes that are partially detrimental to image sensing [5]. This is summarized in Table 1, making it evident that the increasing demands in semiconductor imaging cannot be met with mainstream CMOS technology long after 2000.

As a result, the semiconductor industry started to develop variants of their established CMOS processes under the acronym CIS (CMOS Image Sensing) processes. Such CIS processes continue to profit from the enduring reduction in the feature size of the main-stream CMOS processes. This permits the integration of a growing number of increasingly smaller pixels. The largest semiconductor image sensor fabricated to date contains the impressive number of 111 million pixels, while the smallest pixel pitch reported to date is 1.2 μm [6]. The reduction of the threshold voltage to a current value of about 0.3 V is also beneficial for semiconductor image sensors because the available voltage swing is increased. The reduction of the power supply voltage, however, is a mixed blessing: On one hand, power consumption is lowered appreciably, since it is proportional to the square of the supply voltage; on the other hand, this lowers also the voltage swing for representing photo-signals and, as a consequence, also the dynamic range of the image sensor is reduced.

The replacement of doped poly-silicon as the gate electrode material with silicides ($CoSi_2$ or $TiSi_2$) is beneficial since the gate's electrical conductivity is improved but since silicides are essentially opaque to visible radiation, photosensitive devices employing photogates lose much of their sensitivity. The replacement of bulk silicon with epitaxial silicon layers of a few μm thickness (as in silicon-on-insulator SOI) technology, also reduces the sensitivity of photosensitive devices, in particular in the red and near infrared spectral region where the penetration depth of light in silicon is particularly large. In order to enhance the electrical conductivity of the

silicon substrate, doping levels of the implantations are increased to typical levels of about 10^{18} cm^3. This implies a significant increase of the dark current density to values beyond 1 nA/cm^2 at room temperature. Such values are clearly unacceptable in many imaging applications, in view of the low dark current densities of a few $10pA/cm^2$ in commercially offered CIS processes and the record value of $0.6pA/cm^2$ for the best CCD process.

CMOS technology trend	Eval	Reason
Reduction of feature size	++	More pixels and functionality on chip
Reduction of threshold voltage	+	Higher signal levels and dynamic range
Reduction of power supply voltage	+	Reduced power consumption
	-	Lower signal levels and dynamic range
Gate material: poly-Si → silicides	-	Opaque gates in the visible spectrum
SOI or epi-Si technology	-	Low red response and reduced QE
Increase of substrate doping	-	Larger dark current
Increase of number of metal layers	-	"Tunnel vision"; low QE of small pixels
Reduction of gate oxide thickness	- -	Larger dark current

Table 1. Technological trends on the roadmap of main-stream CMOS technology, an evaluation (Eval) of their positive or negative impact on semiconductor imaging with these processes, and the main reason for this particular evaluation

The combination of shrinking pixel period and increasing number of metallization and via layers results in “chimney pixels”, as illustrated in figure 4, which at the same time reduces the optical sensitivity of the pixels and increase the angular dependence of their photoresponse. Finally, the reduction of the gate oxide thickness to today’s typical values of less than 2 nm increases the tunnel density current through the oxide to values exceeding $1mA/cm^2$, which is clearly unacceptable in image sensing applications.

For these reasons, CIS processes are offered today that are derivatives of industrial CMOS processes, where all the problems mentioned above are addressed appropriately, and where great care is taken that the photosensitive devices can fully profit from the excellent optoelectronic properties of the silicon base material.

An example of pixel layout for a CMOS Active Pixel Sensor is given in Figure 4. Due to the presence of circuitry within the pixel the area that is effectively sensitive to light is reduced to typically 25% - 65% of the total pixel area. This corresponds to the so-called fill-factor. In comparison CCDs typically have fill-factors of 70 - 100% for Full-Frame CCD (FF-CCD) and Frame Transfer CCD (FT-CCD), whereas Interline Transfer CCDs (IT-CCD) achieve fill-factors in the range of 25 - 30%.

A typical cross section of a pixel structure fabricated with such a commercially available CIS process is illustrated in Figure 5. In the silicon substrate photosensitive regions are created using suitable implants: As detailed above, the preferred devices are photodiodes, buried (pinned) photodiodes or CCD structures.

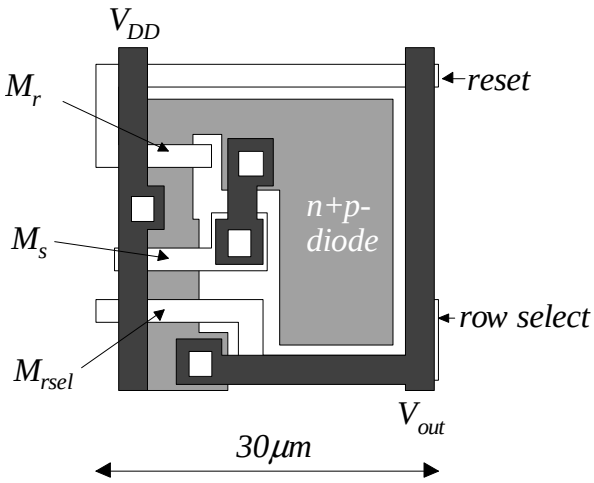

Figure 4. Example of pixel layout for an Active Pixel Sensor

Oxide material is deposited on top of the silicon, containing the copper interconnects and vias, as well as the gate structures for the transistors. Different types of color filters are produced over the individual pixels, followed by microlens structures to enhance the effective light collection efficiency of the pixel. Their focusing effect is illustrated with the broken lines in Figure 5, indicating schematically the ray tracing modeling that is necessary to optimize the optoelectronic performance of the pixels. Typical dimensions of state-of-the art CIS pixels as employed for example in cost-effective image sensors used in mobile phone cameras are periods of 2-3 μm and a total thickness of 3-4 μm.

In order to produce more pixels for less money, the CIS industry will not cease to invest in the continuing reduction of pixel size. This involves solving the problem of reduced capacitance and reduced photosensitive surface of the ever-shrinking pixels: As an example, consider a pixel with a storage capacitance of 1.6 fF; assuming a maximum voltage swing of 1V, such a pixel cannot store more than 10,000 electrons.

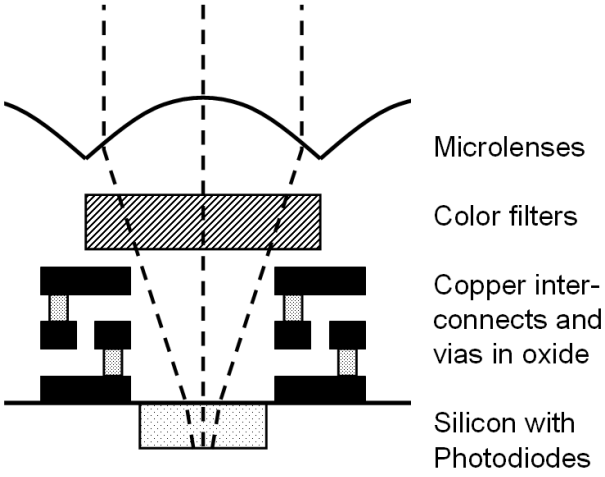

Figure 5. Cross section of a typical CIS pixel, consisting of a silicon substrate with implanted photodiode regions, on top of which oxide material is deposited, where the copper interconnects, vias, gate structures and color filters are fabricated. To improve the light collection efficiency, a microlens array is produced

Since the photogenerated and stored charges show Poisson noise statistics, perceived picture quality deteriorates as a function of the stored photocharge numbers [7]. For this reason, good quality images require photocharge storage capacities of a few 10,000 electrons in each pixel. This problem is quite similar to the one in memory circuits: Despite the continuing reduction of the unit cell size, the capacitance of the unit storage cell must be kept at a certain value, in order to assure reliable operation of the storage function. The solution adopted in CIS technology is, therefore, also related: The third dimension is exploited to increase the specific capacitance of pixel storage devices. An example of this development is the recently developed “stratified pinned photodiode”, realized by corrugating the outer shape of the buried photodiode implant [8].

The other problem of smaller pixels with increased “tunnel vision”, as illustrated in Figure 5, is the reduced photosensitive surface and the increased angular dependence of the response. While microlenses can help to alleviate the problem, there will always remain an angular dependence of the pixel’s response, which reduces the pixel’s overall sensitivity, in particular when imaging lenses with small f/# are employed. A promising technological approach to solve this problem is the separation of the optoelectronic transduction and the electronic circuitry into different layers. This is achieved by depositing a thin film of amorphous or microcrystalline silicon (or another suitable semiconductor) on top of an ASIC structure

(TFA = Thin Film on ASIC technology). Photodiodes are fabricated in the top layer of TFA image sensors, and electrical connections to the charge sensing circuits on the ASIC are produced. In this way, an effective geometrical fill factor approaching 100% can be achieved, and the photoelectric conversion properties, including for example very low dark current, can be optimized separately from the ASIC in the thin film [9].

4 EXAMPLES AND APPLICATIONS OF IMAGERS

4.1 Electronic imaging in the visible spectrum

In the past, the main drivers of electronic imaging have been cost, performance and functionality; without doubt, these drivers will stay unaffected in the foreseeable future. The challenge, therefore, is to take advantage of the continuing progress of semiconductor physics to satisfy the demands of the market in terms of cost, performance and functionality of the realized image sensors and camera systems.

4.1.1 Challenges and opportunities

The key to meeting present-day challenge is integration: More electronic circuitry will be placed on each image sensor, and the pixels themselves will be supplied with all the analog and digital elements to improve their performance and to increase their functionality. Whenever economically justified, an application-specific single-chip digital camera (SoC = System-on-Chip) will result that just needs to be complemented with inexpensive optics to arrive at a highly cost-effective solution.

A first huge, fast-growing and highly contested market is electronic imaging for cell phones. It is estimated that close to one billion cell phone cameras will be sold in 2007. Consequentially, the price of such a complete single-chip digital camera has dropped to less than $5 in volume, while its resolution is already exceeding one Megapixel. From this development, other mass markets such as automotive applications, game console interfaces, personal computer peripherals and videoconferencing will surely profit. Typical single-chip camera developments for these and related applications where price is the main driver are described below.

Two other fast-growing markets with considerably higher margins are digital still cameras (DSC) and security/surveillance. Although both markets combined require only about 100 million image sensors in 2007 – slightly more than 10% of the cell phone camera market – the performance

expectations of the customer are much higher: In the case of DSCs, multi-Megapixel resolution (already exceeding 10 Megapixels even for amateur cameras), high uniformity and low noise are demanded. The performance expectations of the security/surveillance cameras are similar; however, the emphasis is not on the number of pixels but on the low-noise performance for low-light applications. The ultimate physical performance in this respect is single-photon resolution, and as soon as cost-effective solutions will be available, most other electronic imaging applications will demand such a performance, as well. The most promising approaches for low-light semiconductor image sensors are detailed below.

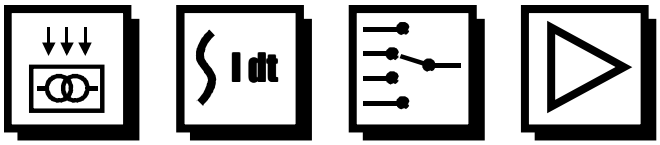

Figure 6. Symbolic functionality of conventional imagers

The third driver of electronic imaging is functionality: In conventional image sensors, the available functionality is restricted to the four basic tasks symbolically illustrated in Figure 6: Conversion of incident light intensity into a linearly related photocurrent, integration and storage of the resulting photogenerated charge packets, sequential access to these charge packets, and amplification/buffering of the signals to make them available off chip. By complementing this basic optoelectronic functionality with analog and digital circuit building blocks, in each pixel or adjacent to the pixel matrix, a very rich toolbox for the realization of application-specific “smart image sensors” is created. Some of this additional functionality, all fabricated with the technological capabilities of the same CIS process, is schematically illustrated in Figure 7, indicating the broad range of building blocks available for the design of custom imagers. This includes, among other things, smart pixels with non-linear response for a dynamic range approaching 200 dB, color pixels making use of the wavelength-dependent absorption of silicon, pixels with unusual geometries implementing selected linear or non-linear transforms, in-pixel analog processing circuits for basic arithmetic operations in the photocharge domain, as well as conventional analog and digital circuits in the pixels or as complementary building blocks beside the photosensor area on the image sensor [10].

The availability of this toolbox of functionality is the key for improving the performance of novel, smart pixels over previous types of pixels, and for providing the custom functionality required for the successful integration of special image sensors for a large variety of applications.

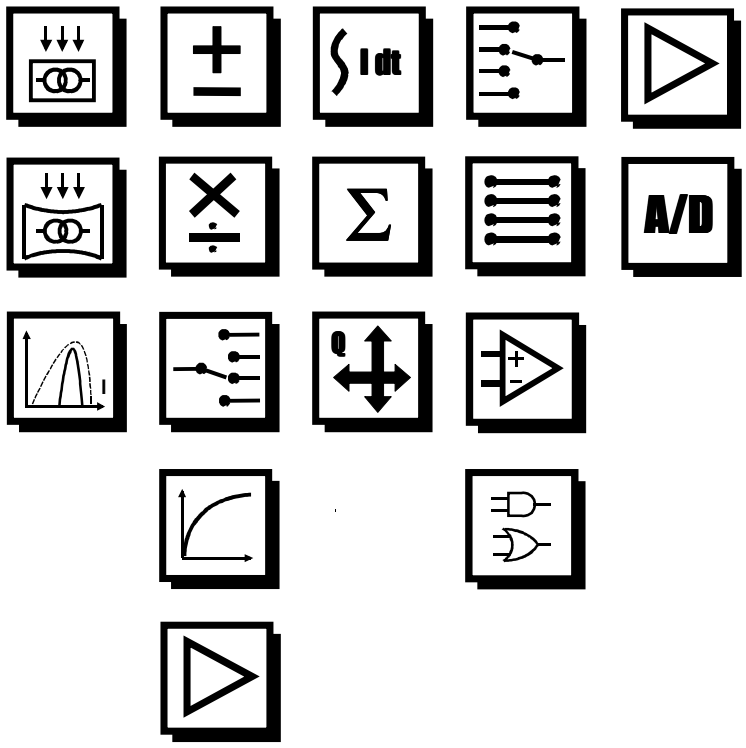

Figure 7. Symbolic illustration of a few examples of functional building blocks available for smart pixels and custom image sensors

As detailed below, this development is expected to culminate in the realization of complete single-chip machine vision systems, so-called “seeing chips”.

4.1.2 Single-chip digital low-power camera

The continuous trend towards miniaturization and higher density in CMOS mixed-signal technologies has a strong impact on the development and progress in solid-state image sensors and related applications. Whereas image sensors based on a passive MOS (Metal Oxide Semiconductor) array architecture were already demonstrated in the seventies, their noise figures and overall performances turned out to be by far not sufficient to compete with dedicated CCD (Charge Couple Devices) based imaging products. It is only with the introduction of the Active Pixel Sensors (APS) concept in the nineties that CMOS imagers have been able to step by step close the gap

with CCDs imagers. The main improvement came with the capability to integrate active transistors within every pixel of the imager in order to locally amplify the typically very small photo-generated signals. This approach basically reduces significantly the large stray capacitances that characterize passive MOS array imager to a few tens of fF, i.e. values similar to the input capacitance of CCDs' output stages. The use of more aggressive technologies and submicron processes was thus instrumental for the performance improvements of CMOS imagers. Furthermore the use of standard CMOS technologies opens up the possibility of manufacturing imaging devices that can be monolithically integrated: functions such as timing, exposure control, and analog to digital conversion (ADC) can be implemented on one single piece of silicon, enabling the production of single-chip digital image sensors. With ever decreasing transistors size, it also becomes technically and economically possible to combine the image sensor with functions such as digital signal processor, microcontroller or further interfaces (e.g. USB). Clearly the higher number of pixels that can be integrated on ever decreasing areas have fuelled the success of CMOS imagers. As such, to a large part, the success of single-chip digital cameras can be seen as a direct result of "more Moore".

Figure 8. Micrograph of a digital single-chip camera with a power consumption of less than

2mW

Today solid-state cameras have become pervasive tools in many markets. It is forecasted that already next year more than a billion solid-state imagers will be sold world-wide, the dominating applications and markets being mobile phones, digital still photography, security, automotive and toys. CMOS technologies and in particular CMOS imagers have also intrinsically

the potential for lower power consumption. CMOS imagers can be driven from one single supply voltage (typically < 3.3 V) and with power consumption below a few tens of mW making these devices particularly attractive for mobile applications, such as the mobile phone market. The latter market corresponds today to roughly 50% of the units sold worldwide.

Low power consumption also helps to reduce the temperature (or temperature gradient) of the sensor chip and camera head, leading in general to improved performances. Figure 8 shows a single-chip digital camera with a spatial resolution of 176×144 pixels. It operates at 1.5 Volts and consumes less than 1mW [14]. The low power consumption is achieved by the reduction in the power supply voltage and by applying special techniques for the analog design. Sensors operating at less than 1mW have also been demonstrated [15]. Video cameras in mobile phone have become a reality today. Undoubtedly further applications, for example in medicine (e.g. minimally invasive medicine / endoscopy) or surveillance and security, will profit from the progress made in low power digital imaging.

4.1.3 High-sensitivity electronic imaging, single-chip digital low-power camera

As we have seen in section 2, the external quantum efficiency of silicon can be close to 100% in the visible spectral domain (for monochrome imaging). Since this means that almost each incident photon is converted into an electron-hole pair, the physical problem of high-sensitivity image sensing is really an electronic problem of high-sensitivity charge sensing. The electronic photocharge detection circuit used almost exclusively in semiconductor image sensing is illustrated in Figure 9: In a p substrate, an n+ output diffusion (OD) is implanted. Using the reset transistor R, this diffusion is reversed biased to a certain reset potential, and it is left floating afterwards. The photocharge Q that should be measured is then placed on OD, lowering its potential by the amount V=Q/C, where C indicates the total effective capacitance at the gate of the source follower transistor SF. The voltage at C in each pixel can be measured individually by connecting SF with the row-select transistor RS to the column signal line Col, which terminates in a load transistor for SF.

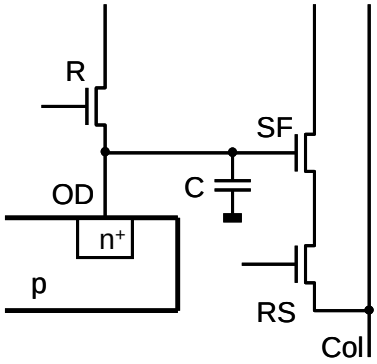

Figure 9. Typical readout structure for semiconductor image sensors

Two noise sources dominate the charge measurement process in the source follower circuit shown in Figure 9: (1) Reset noise – also called kTC noise – introduced by the reset process effectuated by transistor R, and (2) Johnson noise in the channel of the source follower transistor SF. Both effects cause a statistical uncertainty ΔQ (standard deviation) in the measurement of charge packet Q:

$$\Delta Q_{reset} = \sqrt{kTC} \tag{8}$$

and

$$\Delta Q_{Johnson} = C\sqrt{\frac{4kTB\alpha}{g_m}} \tag{9}$$

where k denotes the Boltzmann constant ($k=1.381\times10^{-23}$J/K), T indicates the absolute temperature, B is the bandwidth of the measurement process, α is a constant – with a value not too far from unity – that depends on the way the source follower transistor is operated, and g_m denotes the transconductance of the transistor SF.

For the ultimate high-sensitivity photodetection performance of an image sensor, both of these charge measurement uncertainties must be minimized. Although it has already been demonstrated that single-photon imaging performance can be achieved with several approaches, even at room temperature and at video readout frequencies (corresponding to an output circuit bandwidth of a few tens of MHz), the affordable CIS-compatible single-photon image sensor with at least Megapixel resolution is still elusive.

It is not clear, therefore, which of the various high-sensitivity charge detection approaches will be the winner in this race:

In conventional photodiode-based CIS image sensors, where the output diffusion OD is identical with the photodiode (as illustrated for example in Figure 9), the reset noise described by equation 8 is typically one order of magnitude larger than the Johnson noise in equation 9. With the invention of the CCD principle, it became possible to completely eliminate reset noise by adopting the following measurement sequence: OD is reset to a certain reset voltage and then left floating. The voltage on OD is measured and the value is stored. The photocharge Q is physically transferred on OD, employing the CCD principle, and the resulting voltage drop is measured. The difference of these two measurements results in a voltage value that is linearly related to the photocharge Q, and its statistical uncertainty ΔQ is reduced to the Johnson noise described in equation 9.

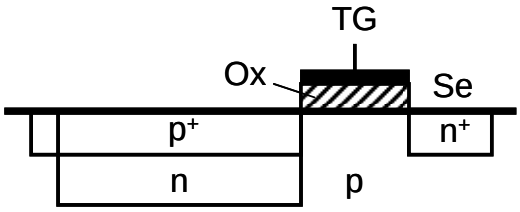

Figure 10. Cross section through a pinned (or buried) photodiode

Since it was believed that it is not possible to transfer a stored amount of charge from one diffusion (e.g. a photodiode) to another one (e.g. the OD in Figure 9), without introducing additional noise, CCD image sensors were considered superior in terms of noise performance compared to imagers fabricated with CMOS-compatible processes. A conceptual breakthrough occurred with the invention and the fabrication technology of the pinned (or buried) photodiode (PPD), illustrated in Figure 10.

As shown in this figure, a buried n-type volume is entirely surrounded by p-doped silicon. This PPD can be fully depleted, so that CCD-type operations such as complete charge transfer using the transfer gate TG become possible. This implies that image sensors fabricated with CCD as well as CIS technology can reach the Johnson noise limit described by equation 9. Using this approach, a charge measurement noise of less than 10 electrons r.m.s. can be obtained in practice.

For the past two decades, researchers have grappled with the Johnson noise equation, with the aim of attaining single-electron photocharge detection noise in an image sensor at room temperature and at video frequencies (corresponding to a readout bandwidth of 10-20 MHz):

- The effective capacitance C can be reduced to values below 1 fF using double-gate field-effect transistor (DG-FET) technology. Although single-electron noise is achieved, it comes at the expense of complex technology modifications and voltages above 20V.
- A similar approach with buried charge modulation devices (BCMD) results in charge noise values of a few electrons, again requiring complex technology modifications.
- CCD image sensors used for astronomical applications are read out at very low frequencies of around 50 kHz, and they are cooled down to about -100^0C. This results in single-electron noise performance but at the expense of very long readout times.
- The so-called Skipper CCD is operated at room temperature, using floating gate readout structures to measure the same photocharge repeatedly in a non-destructive way. The averaged measurements show the desired single-electron charge noise but the necessary averaging over more than 100 individual measurements per pixel slows down readout significantly.
- In order to circumvent the problem of noisy electronic charge detection, physical amplification mechanisms with low excess noise factors are actively pursued. Image sensors with avalanche photodiodes (APD), either working in the linear or in the Geiger mode, have been realized, exhibiting the wanted single-electron charge noise at room temperatures and at video frequency readouts. Several products such as the Impactron™ CCD image sensor with avalanche amplification section, developed by Texas Instruments, are offered commercially. Unfortunately, the high electric fields required to cause avalanche amplification still necessitate voltages of 20V and more, making the use of avalanche-based single-electron imagers somewhat unpractical.
- Probably the most promising approach for cost-effective single-electron image sensors is “bandwidth engineering”: The measurement bandwidth B in equation 9 is significantly reduced, either at each pixel site or in each column amplifier. Suitable imager architectures with parallel readout capabilities provide for data readout at unimpeded speeds, despite the low-pass filtering effect, see for example [11]. The large advantage of this approach is its entire compatibility with standard CIS technology, as well as low-power, low-voltage operation.

None of these approaches has yet resulted in the commercial availability of cost-effective, easy-to-use image sensors with close to single-photon performance. Without doubt, such devices, based on one of the described principles, will become available in the next few years.

Pixel dimension reduction is justified not only to decrease the costs, following the Moore's law trend, but also to reduce the volume and thickness of the imager including its optical part. The reason is that for a given optical f#, a reduction of the lens diameter results in a reduction of the focal length and hence to the total thickness of the imager. The main drawbacks of this trend concern the optics, with diffraction effects close to the pixel pitch, and the pixel collected charge possibilities, reduced as the pixel size is lowered. The drastic size reduction of the well collecting the photogenerated electrons, able to collect typically 40'000 e- with 16µm in pitch pixel, 10'000 e- with 2.2µm and 6'000 e- with 1.45µm, is the strong motivation to decrease the total noise coming with each pixel reading: the dynamic range being reduced with its upper limit, the lower limit must improve drastically. The best read noise results are now in the range of 1 to 2 electrons RMS. Nevertheless, even with a low noise reading, the fluctuations of photogenerated electrons number is correlated with a Poisson distribution, which predicts a RMS value given by the square root of the total electrons number. This phenomenon comes from the photon number statistical fluctuation, and cannot be avoided without increasing the total number of collected electrons. To obtain a SNR (Signal on Noise Ratio) of 10, 100 photogenerated electrons are necessary with a perfect non-noisy reading circuit. To increase this collection number, several directions are to be considered.

SNR limitations come primarily from the optics size; a lower f# is necessary to both lower the diffraction and increase the collected photons. This leads to large incident angles not compatible with the path through interconnection layers, as illustrated in Figure 11.

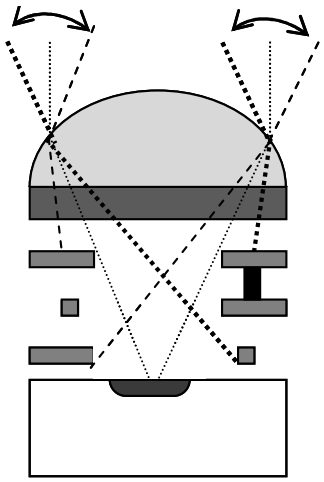

Figure 11. Light path through interconnects for large optical aperture (low F#)

To overcome this limitation, large angle collection is provided by back-side and thinning approaches. This technique, yet used for high end CCD products for space applications, provides high fill factor, high photon collection angle and improved pixel crosstalk. This technique is based on wafer bonding and thinning, and the thin top silicon layer, necessary to collect efficiently the photo generated electrons, is difficult to obtain and passivate. One way is to use a SOI substrate, allowing to keep the initial buried oxide as the top final passivation layer, for high quality interface and controlled Silicon thickness: this back-side technique is illustrated in Figure 12. Another way is to improve the thinning control to reach the desired value, and to passivate to the final silicon surface by the use of laser anneal and low temperature deposition.

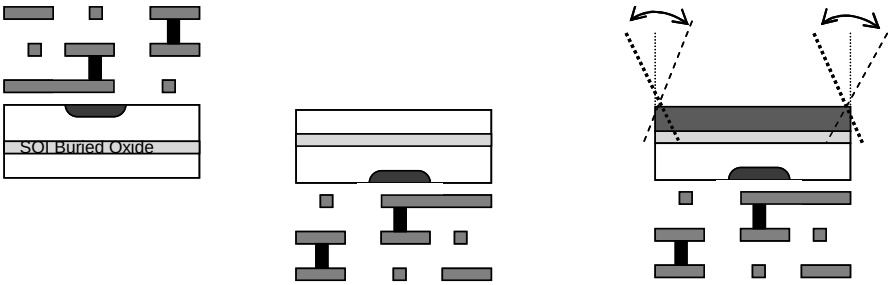

Figure 12. Back side technique to overcome the light path screening through interconnects for large optical aperture (low F#)

4.1.4 Color imaging

Appropriate color restitution requires that the color recording is as reliable as possible. Human sense of color is based on a triplet cells in the eye's retina: the spectral sensitivity of these 3 types of cells is the base of the color recording. Color science, as investigated by the CIE (Commission Internationale de l'Eclairage), gives the rules to achieve good restitution of the available colors in the world, as seen by the human eye. The main result is as follows: the reconstruction of all colors is possible if for each image point 3 different light intensity measurements are acquired, these measurements having relative spectral sensitivities given in Figure 13, or linear combinations of them.

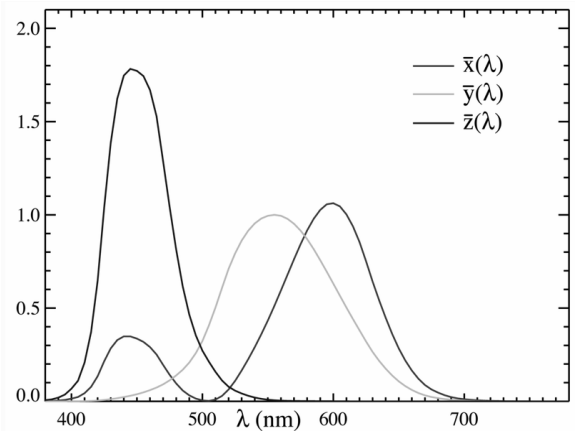

Figure 13. Normalized spectral sensitivities allowing reliable reconstruction of all colors

The classical way to obtain these spectral sensitivities is the use of color filters. They are made of photoresist layers deposited on top of the imager circuits, as previously shown in Figure 13. Three types of photoresist, e.g. Red, Green and Blue are necessary; complementary colors could be used as well; they are generally deposited in a 2x2 pixels pattern known as the Bayer pattern (Figure 14).

Figure 14. Bayer pattern for color filters

The limitations of this technique are:

- The thickness of the resist, around 800nm, becomes high with respect to the width of the pixel. Thinner filters would lead to reduced optical aberrations due to lateral optical path from the top surface to the silicon

- The maximum temperature allowed by the resist is much lower than any other layers in the circuit: no high temperature process step can be done after color filter deposition
- The filters absorb around 2/3 of the incoming light; this is a main cause of loss of photons and thus sensitivity
- The three types of color sensors are not at the same location, resulting in some color reconstruction difficulties and aliasing/Moiré effects

To overcome these limitations, several techniques have been investigated. The 3 types of sensors can be arranged vertically, i.e. using stacked photodiodes as demonstrated by Foveon: it uses the light absorbance variation in silicon to detect the red signal deep into the silicon, while red and green signals are absorbed closer to the surface and finally red+green+blue signals are detected in the top p-n junction that is located closest to the surface of the silicon. An alternative technique consists in using mineral filters integrated in the CMOS process. This leads to a higher temperature resistance and a thinner total stack thickness, thus lowering the lateral shift of photons causing diaphoty. More recently the use of the filtering behavior of submicron metal patterns creating plasmons when impacted by light has been envisioned and is currently been investigated.

4.1.5 High-speed image sensing

High-speed imaging allows motion analysis in various application fields such as scientific measurements, machine vision or holographic data storage to mention a few. Impressive application examples are available from various suppliers [16].

In a broad sense, image sensors can be considered as “high-speed” as soon as they exceed video rates (over some 60 frames per second (fps)). The “speed” (maximum frame rate) of an image sensor is closely related to its spatial resolution and more particularly to its number of rows. For example, a sensor capable of 1’000fps while scanning 1’000rows (row-rate = 1us) is able to deliver 10’000fps when scanning a partial image of 100rows (row-rate =1us). The reason why the number of columns has almost no impact on the sensor frame rate is that the majority of today’s high-speed sensors use column parallel readout circuitry.

The highly parallel architecture of CMOS sensors has led within the last decade to a technology shift from CCDs towards CMOS imagers for high-speed imaging. For low spatial resolution in turn, CCD sensors are still capable of recording high speeds, which have by far not been equaled by

CMOS. As a comparison, a 320×260pixel CCD sensor using *in situ* storage is capable of 1M (10^6) fps [17], while a 352×288pixel CMOS sensor using innovative *in situ* ADCs reaches 10k (10^4) fps [18]. For higher spatial resolution (and lower speed) CMOS image sensors (CIS) have however overtaken the market place. This success is mainly attributable to the system integration capability of CIS, which leads to lower cost cameras. Up to the 1990's, CCD- and early CIS [19] delivered analog output and thus A/D conversion had to be performed in separate ICs. With the advent in the late 1990's of the first on-chip column-parallel ADCs [20], the way was paved for implementing high-speed / high resolution digital imagers [21]. Today, a typical 1.3 Megapixel high-speed sensor delivers 500fps at full resolution [22].

To speed-up image acquisition, high-speed sensors use snap-shoot pixels operating in the "Integrate-While-Read" (IWR) mode of operation. IWR-capable pixels do per definition require *in-situ* storage, a property that was interestingly also required in the very first CMOS photodiode array published in the early 1990's [23]. Therefore, the same 5T pixels where re-used [19] and fine-tuned for improved responsivity [24], one of the key requirements to the sensing part of a high speed sensor, since high frame rates imply short integration time. To improve the sensitivity at pixel level, the conversion factor (CF) must be maximized, e.g. the capacitance of the photodiode and floating diffusion must be minimized. With the 3um process in the early 1990's, C_d and C_{FD} where in the order of 50fF [23], yielding a poor CF of ~1.6µV/e-. With a modern 0.25um process, a CF of 13µV/e- is typical [22], meaning that C_d and C_{FD} have been lowered to some 6fF. Various pixels with improved sensitivity have been proposed by either incorporating an amplifier in front of the shutter [25] [26] [27] or an in-pixel charge amplifier [28]. The first approach improves CF by a factor of 2 (~20µV/e-), while the second allows boosting the CF to some 38µV/e-. With the advent of pinned photodiode, the CF of traditional 5T pixels improves by a factor of 2, which allows smaller pixels [29] to rival with more complicate ones in term of CF. In addition to CF improvement at pixel level, almost all sensors further increase the overall sensitivity by electronic gain boosting inside the column amplifier (prior to A/D conversion).

Three types of column-parallel ADCs are used in today's CIS: single-slope, successive-approximation (SA) and cyclic/pipeline converters. Single slope converters are widely used in low-speed imagers. Recently, however, such an ADC has been pushed to a remarkable speed of 180fps at 1440rows (row-rate = 3.86µs) for 10bit by using a 300MHz clock [30]. Sensors with higher throughput usually use SA-ADCs, which typically reach 5000fps at 512rows (row-rate = 0.39µs) [24] or 440fps at 1728rows (row-rate = 1.3µs) [31] for 10-bit. It is difficult to achieve more than 10bit grey-scale resolution

with SA-ADCs on CIS. To increased the ADC resolution, the authors of [28] have developed cyclic converters capable of 3'500fps at 512rows (row-rate = 0.56µs) for 12 bit. Other publications have reported the use of multiplexed pipeline converters [27] [32] with similar aggregate performances as early-days SA-ADCs (500fps at 1024rows / 2µs row-rate for 10-bit [32] [21]).

High-speed digital CIS produce tremendous amounts of data: for example, the 440fps 4.1Mpix sensor of [31] delivers 18Gbit/s (4.1Mpix×440fps×10bit), which are dumped into some external IC over 160 pins toggling at 120MHz. Such I/O bandwidths are indeed quite challenging to handle both at IC-level (large power consumption, on-chip noise) and at board-level (large buses, signal integrity). Some newer designs thus propose LVDS outputs [33] [27] [32] to solve those issues. Recently, incorporation of on-chip parallel image compression circuits for reducing the data traffic has been proposed [34]. In a prototype 3000fps sensor, a compression ratio of 4.5 has been demonstrated.

In future, further functionality will be integrated onto CIS dies. An example of such a sensor using programmable single-instruction multiple data-stream (SIMD) parallel digital processing has been published in [35]. The IC, aimed at high-speed machine vision, combines image acquisition, digitalization and column-parallel SIMD processing with a computational power of 100 GOPS. With the availability of sub 100nm mixed DRAM/imager technology, integration of a frame memory will also become economically viable [34].

4.1.6 Optical time-of-flight 3D cameras

Humans are capable of perceiving their environment in three dimensions. This key capability represents in turn a major challenge to film-based and electronic camera systems. In fact so far, cameras have been typically optimized for, and also limited to, the acquisition of two-dimensional images, providing basically only monochrome or color images without any direct information on depth. The race for higher (lateral) spatial resolution continues unabatedly; today's still picture cameras for the consumer market offer resolution in excess of 10 Megapixels, whereas scientific and professional cameras already counts more than a few tens of Megapixels. This race for more pixels is very reminiscent of the continuous trends towards a higher degree of integration, a higher number of transistors as described by "more Moore". In contrast the shift from 2D imaging toward real-time 3D imaging represents a major technological step and paradigm change. A new type of information is available, based on sensors and pixels with added functionality thanks to processing capabilities (at the pixel level). These smart sensors and pixels can be seen as vivid examples of "more than

Moore". It also opens up completely new applications opportunities in numerous fields such as in security, in automotive, in industrial control and machine vision, in the medical sector as well as in consumer electronics and mobile robots. All these applications can very directly benefit from camera systems that are able to capture the world in real-time and in all three dimensions. This is particularly true if such 3D systems can be made compact, robust and cost-effective. The technological requirements for such 3D systems are nevertheless stringent: To a large extent obtaining reliable real-time distance information over an entire scene is indeed very challenging and originally distance measuring systems have been limited to point measurements or to scanning systems, the latter being rather slow and/or expensive. Over the last few years however, technological progress in semiconductor devices and micro technologies have lead to sensors that can "see distances" within complete scenes at affordable prices [36, 37, 38, 39]. The breakthrough came with a new type of optical 3D camera based on the time-of-flight principle that uses the finite velocity of light (c = 3× 10^8m/s) to measure distances. Either a pulse or a continuously modulated light wave is sent out by an illumination module. Correspondingly, either the "time of flight" t - that is the time the light needs to travel from the illumination module to the target and back to the sensor -, or the phase delay ϕ of the continuously modulated light wave for this roundtrip is used to calculate distances within a scene. The latter method, referred as continuous wave (CW) modulation presents several advantages over the light pulse technique. In particular the requirements to the illumination module and the electronics are not so demanding. Short optical pulses require a high optical power and a high bandwidth of the electronic components. In the CW modulation scheme, light from a LED or laser diode array is modulated to a frequency f_{mod} of a few tens of MHz and illuminates the scene. The light which is reflected back by the objects and/or persons in the scene is imaged with a lens onto a custom solid-state image sensor. Each of the pixels of this sensor is capable of synchronous demodulation of the incident modulated light, for the precise local determination of the phase delay. From the phase delay ϕ, distances can be computed directly as given by the following equation.

$$L = \frac{L_0}{2\pi} \cdot \phi \quad \text{with} \quad L_0 = \frac{c}{2 f_{\mathrm{mod}}} \text{ the unambiguous range} \qquad (\mathbf{10})$$

Current sensors achieve distance resolution in the mm range for distance up to a few meters in real time. Camera systems providing lateral resolutions of up to 176×144 pixels are commercially available today [40]. Higher resolutions up to 360×240 pixels have been demonstrated [41] and products with spatial resolution of up to VGA are expected in the near future. Figure

15 shows a sample image of a person entering a room. The information on the depth allows typically distinguishing reliably and effectively objects and persons from the background of the scene. In fact the acquired 3D image data enables the very simple extraction of important information, such as the position and distance of objects and/or persons in the scene. This type of information turns out to be often key, in particular to human beings in solving many day to day tasks as well as more complex tasks. Thanks to 3D cameras, many applications in the field of automation, security, etc… are expected to profit as well from this 3D seeing capability.

Figure 15. Sample image of 3D data (with permission of Mesa Imaging) [40]

4.2 Beyond the visible spectrum

Since imaging is performed in most cases by means of electromagnetic waves (magnetic resonance and ultrasound imaging are ignored within this document), the key parameter is the wavelength used. Visible imaging enables to cover all applications where the information needs to be close to the human vision. Beyond the visible spectrum, X-ray, infrared and terahertz electromagnetic waves are of most interest in many applications.

4.2.1 Challenges and opportunities

Medical imaging, for example, is accomplished by means of X-ray, gamma rays (in nuclear medicine), visible light (ocular fundus, skin), infrared light (mamma transillumination), or even terahertz waves, which has been proposed recently. In breast X-ray imaging, the gold standard is the X-ray-based mammography, where a special radiographic unit is used. Optical imaging of the retina is the only way to examine veins directly and non-invasively. Tele-ophthalmology has been demonstrated in a large international project.

Medical imaging, industrial control, and surveillance applications really take the benefit from detector innovations for the X-ray range (example CdTe material developments and new hybridation technology), infrared technologies (continuous need for improvement to decrease price), and new terahertz technologies.

4.2.2 X-ray imaging

Today X-ray imaging is used in many domains: medical, non destructive testing, and security check. Most of the new developments are currently driven by medical requirements. This paragraph aims at giving a specific focus on medical image sensors.

First based on films, in the 1970s analog fluoroscopy became widely used. This modality was realized by an X-ray image-intensifier tube coupled to a TV camera. Sometimes, this kind of system was also used to take single images where the image resolution, however, was limited by the camera performance. In the 1980s, X-ray radiography became digital by introducing the so-called computed radiography where a storage phosphor in a cassette is irradiated and later on read out by a laser scanner.

State-of-the-art all-digital X-ray imaging is accomplished by flat-panel detectors.[2] These detectors are based on a large-area semiconductor film, i.e. hydrogenated amorphous silicon (a-Si), forming an array of thin-film transistors (TFT) managing readout of the picture elements. The fundamental interaction of the electromagnetic radiation with the material is absorption, which is dependent on energy. Secondary effects are reflection, scattering, diffraction, and refraction. All these interactions can be studied with Monte Carlo simulations. Details of interest differ from the surrounding tissues. This results in a contrast. In order to "see" its amplitude, it needs to be compared with image noise.

The total image noise includes the detector noise. Therefore, it is still of great interest to work on the performance of such X-ray image sensors

4.2.2.1 Current digital X-ray image sensors

Current digital X-ray imagers are FD detectors (Flat-panel solid state Detectors), which are suitable for most X-ray imaging applications. They are based on an amorphous silicon a-Si readout matrix; each pixel comprises an a-Si switch and a sensing element. The restricted space limits the resolution to a minimum pitch of some 70 µm.

For better resolution, the most advanced X-ray image sensors are CCD or CMOS based. The pixel size can be as low as 10µm×10µm. These image sensors are responsive in the visible range. For X-ray imaging, the conversion from X-rays to light is performed by a scintillator coupled to a fiberoptic face plate. This configuration leads to the best resolution (better than 20 lp/mm).

Large surfaces up to 49mm×86mm are currently commercialized. However, CCDs and CMOS have reached their limits, i.e. increasing the surface in such technologies is hardly compatible with reasonable production cost.

For large field of view, e.g. for X-ray imaging such as mammography, chest imaging, and computed tomography, it is important to work on new large sensors.

4.2.2.2 New image sensor concepts

In recent years, several advanced imaging solutions have been realized or are currently under development. In the following, some of these technologies are presented.

CCD-based detectors for very high spatial resolution: As mentioned above, FD detectors are suitable for most X-ray imaging applications. They are based on an a-Si readout matrix, each pixel comprising an a-Si switch and a sensing element. The restricted space available leads to a minimum pixel pitch of some 70 µm, otherwise the spatial fill factor of the pixels

would become too low. Especially for mammographic biopsies, imaging with very high resolution is desirable. Therefore, a CCD-based detector has been developed with a pixel pitch of 12 µm. It can be also used in a 2×2 or 4×4 binned mode, resulting in 24 or 48 µm pixels, respectively. The detector uses a CsI scintillator which is coupled via a fiberoptic plate to the sensor with 4k×7k pixels. The sensitive area is 49mm×86mm being the largest CCD in serial production in the world [8].

CdTe is also a material of choice. Up to now, price versus performance were questionable, but current R&D efforts performed on both, material growth (in order to improve yield and size) and hybridization technology (in order to decrease the pitch and hybridization cost), give good results and open new perspectives for this material (e.g. X-ray intra oral application) for medium size imaging. This technology should increase drastically the image contrast and aim at being compatible with market price.

Organic semiconductor-based detectors: Current FD detectors are based on a-Si technology that has proven to be suitable for radiologic, fluoroscopic, and angiographic applications. These detectors are built on glass substrates which are rigid, heavy, and fragile. The a-Si layers and electrodes are patterned by photolithography, a process enabling the production of fine structures. Depositing a-Si requires elevated temperatures in the order of 250 °C. In summary, there is also a demand for cheaper alternatives to a-Si technology.

Some investigations are going on into all-organic detectors.[9] Plastic substrates can be used which are flexible, light-weight, and unbreakable. The organic semiconductor and electrode layers can be deposited in the desired pattern, e.g. by jet printing. This results in cheap detectors which have the potential for new applications. Since an organic detector is not as heavy as an a-Si-based detector, it is qualified to be used in a portable bed-side device.

It has been demonstrated that organic photodiodes and transistors are feasible, but further work is necessary to improve their performance.

4.2.3 Infrared image sensors

Today thousands of cooled IR detectors are produced taking advantage of the good know how regarding this domain [1] [2] [3] [4]. However these current IR detectors have some limitations regarding their ability to operate in all weather conditions, and in terms of compactness and reliability. Therefore research for moving to the next generation of detectors are in progress to overcome these limitations as well as to offer more performance. In parallel, the production cost reduction is one of the main challenges for cooled IR detectors and new technologies are developed to answer this need.

These new researches and developments are dedicated to smaller pixel pitches; large formats, avalanche photodiodes (APD), multicolor detectors and active imagery detector needs as well as optimization of microbolometer technology, one of the best choice for compactness/ very low price compromise. This technology still requires miniaturization but is very promising and should open new applications in volume markets such as automobile and energy monitoring in buildings.

4.2.3.1 Infrared detector development

A lot of different technologies and sensitive materials are well mastered and available for IR detector production. As a matter of fact, quantum well IR photo detectors (QWIP) have been developed (ex Thales Research and Technologies (TRT)) and are at mass production level in cooperation with Sofradir. Then InSb technologies are also available.

As to HgCdTe technologies, they have been widely used for high performance IR detectors and are at mass level production for years. Finally uncooled technology was developed based on amorphous silicon microbolometers at CEA- Leti. Then it was transferred to ULIS (the subsidiary of Sofradir) and is at mass production level since 2003. In addition other developments are running like InGaAs technology in Xenics and III-V lab.

The mastering of all these technologies in Europe shows leading position in Europe for the present generation but also for the next generation in development. These different technologies are complementary and are used depending on the needs of the applications mainly concerning the detection range needs as well as their ability to detect in bad weather environmental conditions. They can be classified as following (see Figure 16):

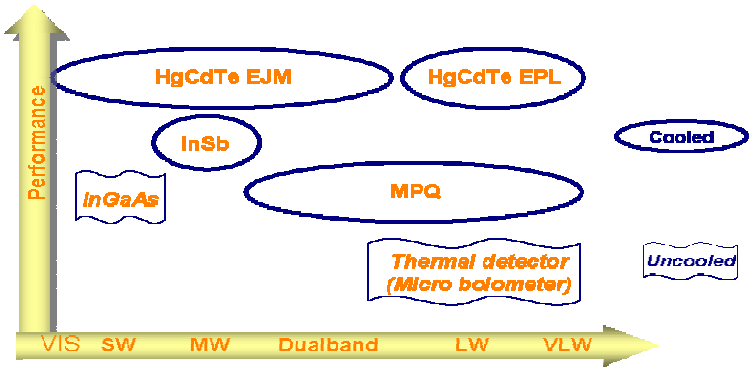

Figure 16. Different IR detector technologies

- **High performance IR detectors for long range detection systems:** Long range detection systems are dealing detection ranges ranging from 6 km to tens of kilometers. High performance detectors are necessary for long detection range and will also be necessary for scientific, applications including spectrometry, where you have very small signal (or emitted flux) to detect. For these applications high performance cooled technologies are mandatory and mainly both HgCdTe and InSb can reach today these detection ranges.
  - HgCdTe material: based on the unique characteristics this semiconductor, MCT IR detectors can be sensitive in a very large range of wavelengths, starting from visible up to about 18 µm. These detectors exhibit high quantum efficiency coupled with high signal to noise ratio and can be operated at a rather high operating temperature compared to concurrent cooled technologies.
  - In addition high productions capacity and low cost are possible with the new growth method (Molecular Beam Epitaxy / MBE) for short wave (SW) and medium wave (MW) bands as well as
  - for dual band SW/MW and MW/MW. For long wave and very long wave band the classic Liquid Phase Epitaxy (LPE) will continue to be used in the coming years. Finally this material offers a large range of improvements regarding APD and dual band devices which confirms that it is dedicated to high performance systems.
  - InSb: this semiconductor is just sensitive in the MW with a fixed cut-off band at 5.5 µm at 77 Kelvin, and there are presently some technological limitations in operating temperatures as well as in pixel pitch reduction. Consequently, performance obtained may be limited in some demanding applications.

Quantum well photoconductors (QWIP) may also be used for long range in some specific case but with very low detector operating temperatures and low imaging frame rates.

- **IR detector for medium ranges detection systems:** Medium detection ranges are dealing with few km to about 6 km maximum. For these applications; medium to high performance cooled technologies are also mandatory. As a matter of fact, in some cases, the use of high performance detector can allow an IR system cost reduction (reduction of optics size, simplification of signal processing, relaxation of reliability constraints…). Consequently the different candidates could be the same than for long range but in some cases, QWIP for LW and InGaAs for SW, can offer a good quality / price ratio.

- QWIP: there are mainly used for LW range but they have a limited efficiency as well as a higher dark current than concurrent high performance technologies, which limits their performance.
- InGaAs: it is mainly used in short wavelength range and it is in production up to about 1.9 µm cut-off. For very low input signal they may be limited by the readout circuit noise performance.

- **IR detectors for short range detection system:** Short detection ranges are dealing with few hundred of meters to 1 or 2 kilometers at maximum and uncooled technologies answer these needs with uncooled operation. The most successful technology offering the best quality/price ratio is the micro bolometer one based on amorphous silicon which is fully compatible to CMOS silicon technology.

4.2.3.2 Focus on microbolometer technology

The principle of the microbolometers relies on the heating produced by the incident infrared radiation.

Thus the measurement is indirect and involves a temperature variation sensitive element: the thermometer. The scene at a temperature T_{sc} emits an infrared light through an optics and is converted by an absorber in order to heat the thermometer.

Radiation power is however very low and thus thermal insulation of the thermometer with respect to the readout circuit is of most importance.

Absorption can be performed directly within the thermometer itself and it can be further increased thanks to a quarter wave cavity arrangement. At this point the bolometer is built as a thermometer with infrared antennas.

The thermometer can be realized using different principles: pyroelectricity, ferroelectricity, thermopiles or variation of resistors.

The readout circuit then translates heating into voltage or current.

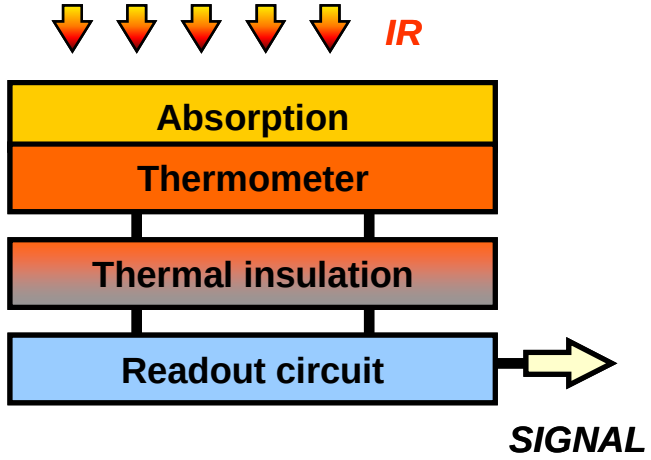

Figure 17. Bolometer principle

From a device point of view, the evaluation of the quality of a bolometer is provided by the Noise Equivalent Temperature difference NETD.

The response is the variation of the output signal ΔI_{signal} with respect to the scene temperature variation ΔT_{sc}:

$$\text{Response} = \Delta I_{signal} / \Delta T_{sc}$$

The NETD is the noise equivalent at the input of the device:

$$\text{NETD} = I_{noise} / \text{Response} = I_{noise} \cdot \Delta T_{sc} / \Delta I_{signal}$$

Considering now the particular technology developed at LETI, the pixel features a microbridge structure, which affords a very high thermal insulation of the sensitive part of the sensor from the readout circuit. This sensitive part is made from a thin film of amorphous silicon . The proper design of the support legs provides the required thermal insulation, while it also ensures the mechanical strength and electric connection of the thermometer. To further improve the thermal insulation, the sensor is packaged under vacuum.. Although the elementary module represented here measures 50 µm by 50 µm, IRFPA with 25µm pixel are now totally affordable, and latest developments are now focused on 17µm pixel achievement.

On top of the readout circuit a reflector is deposited. It forms with the electrodes a quarter wavelength cavity for a wavelength of 10 µm and it boosts the absorption by creating a maximum intensity at the detector level.

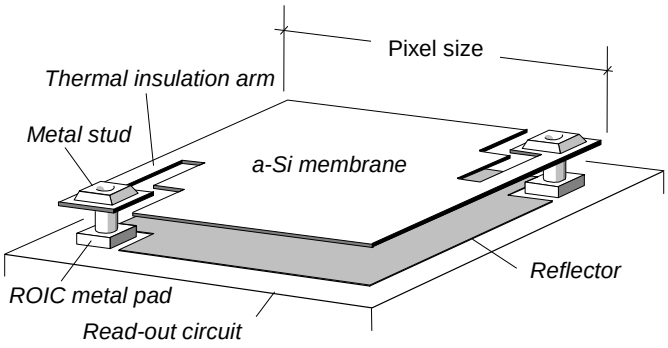

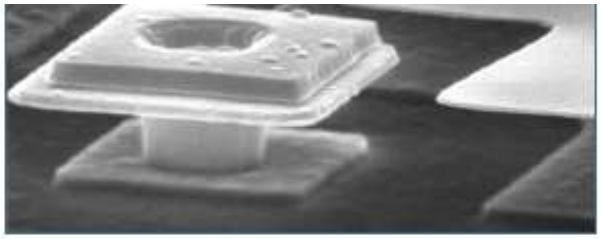

Chapter 8

Figure 18. Pixel architecture

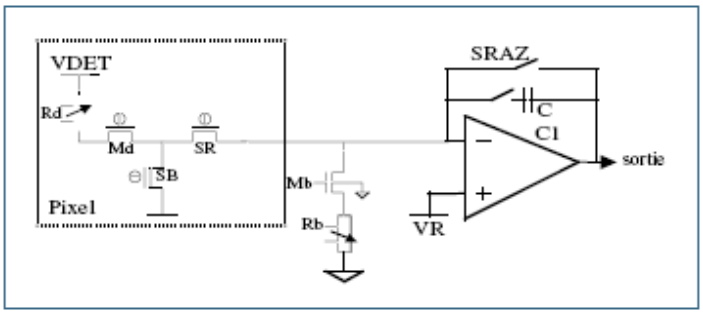

Figure 19. Zoom on the contact between readout circuit and thermometer

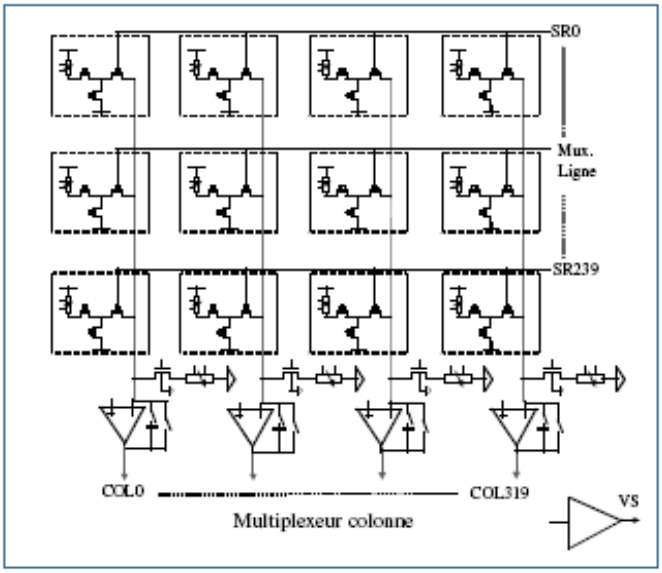

Figure 20. 2D microbolometer readout circuit architecture

Absorption of such a structure while considering that the reflector and the electrodes are separated by vacuum is:

$$\varepsilon(\lambda) = \frac{4\frac{R_{\square}^{vide}}{R_{\square}}}{\left(1+\frac{R_{\square}^{vide}}{R_{\square}}\right)^2 + \cot^2\left(\frac{2\pi d}{\lambda}\right)}$$

With $R_{\square}$, resistivity of the electrodes, $R^{vide}_{\square}$, the resistivity of the vacuum layer ie: 377 Ω/□, d, distance between the reflector and the electrodes and λ, the wavelength. The maximum value of ε is obtained for a resistivity of the electrode layers equal to the vacuum. In these conditions the device is called adapted.

Absorption modelization of such Fabry Perrot cavity is widely described in the literature.

4.2.3.3 Focus on MCT

Hg(1-x)CdxTe presents unique properties that make it an ideal candidate for most of the needs in infrared detection in all the IR spectral bands.

Firstly, the band gap can be tuned by just controlling the xCd/xHg ration of the alloy, making possible the entire infrared band to be covered from visible to very long wavelengths. (Zero band gap for xCd :0.15) as presented in figure 21A.

Secondly, the lattice parameter doesn't change at the first order from CdTe to HgTe. This allows the use of lattice matched CdTe substrates. Cd(1-y)ZnyTe is the more extensively used today for its better quality and because it leads to a perfect lattice matching by adjusting at the second order with yZn composition to the xCd composition. Very high quality epitaxial layers of Hg(1-x)CdxTe can be grown today on very high quality Cd(1-y)ZnyTe oriented substrates with a crystallographic quality similar to the substrate.

The very small lattice parameter variation versus composition makes also possible the fabrication of lattice matched multilayer epitaxies with only a very small amount of defects and dislocations. Today, very high quality Hg(1-x)CdxTe/ Cd(1-y)ZnyTe epitaxies can be grown either by liquid phase epitaxy or by vapor phase epitaxy (molecular beam epitaxy for example).

This semiconductor can be doped n-type (for example with Indium) and p-type (by mercury vacancies or Arsenic) making possible n on p or p on n junctions to be fabricated.

Fundamental parameters such as lifetime are relatively high leading to low dark current and large quantum efficiency (near 1) photodiodes. Moreover the performances of detectors are only limited by the physics and predictable by validated models in a large domain of temperatures and compositions (see *Figure 21*B).

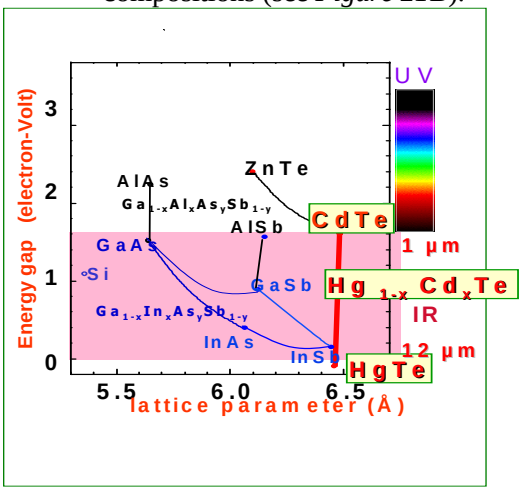

A

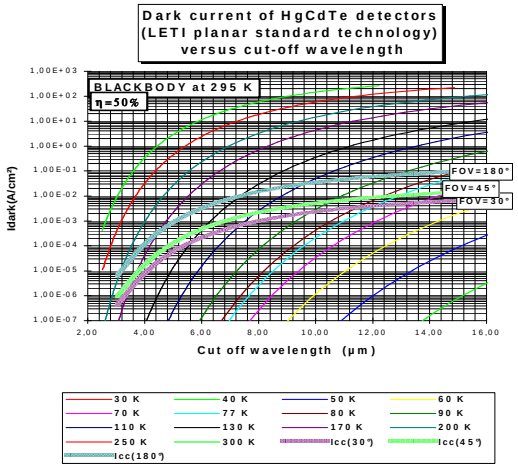

B

Figure 21. A/ Lattice parameter of HgCdTe versus composition

B/ Dark current model for n on p photodiodes for cut off wavelengths from 2µm to 16µm and operating temperature from 30 and 300K

This very large flexibility of these alloys makes possible:

- the fabrication of a large variety of infrared detectors , in particular multicolor detectors which need multilayer epitaxies.
- to adjust the composition of the alloys to the useful infrared band to get the ideal composition xCd / operating temperature couple to get the optimum performance for the focal plane array.

Among the other advantages recently pointed out we can mention:

- an optimum light collection in backside illumination from the cut off of the detector to the near UV, including the entire visible spectrum, without any decrease of quantum efficiency.
- A unique specificity in the semiconductor field for MCT avalanche photodiodes that can exhibit very large gain at moderate bias, without any excess of noise (F(K) strictly equal to 1).

All these properties allow this semiconductor, to answer all the high performance needs and classes of detectors in infrared bands up to at least 20µm.

4.2.4 Terahertz image sensing – new concepts

The terahertz part of the spectrum has recently been investigated. The ability to detect metallic parts under clothes without an ionization source is seen as being the answer to increased screening airport controls after 01/09/11.

Currently, no cost effective industrial solution exists and thus detectors are still at early development research & development stage.

Up to now, several kinds of detectors have been studied worldwide for terahertz sensing. The following table summarizes the available devices: it was displayed by VTT in Finland and shows a THz detector classification of existing technologies. This classification stresses on three major issues: sensitivity, frequency range and price.

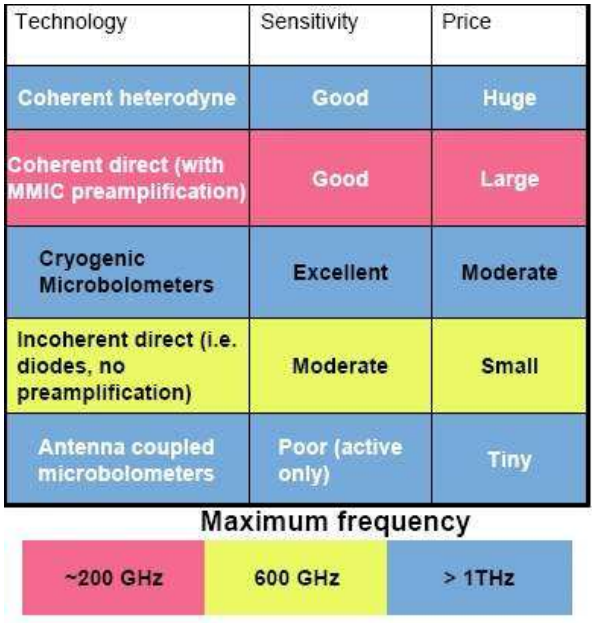

Figure 22. Existing THz technologies (VTT)

Since last ten years, all R&D efforts spent in Europe were performed on MMIC (Monolithic Microwave Integrated Circuits), heterodyne detection, cryogenic bolometer. These technologies exhibit a major drawback: they can not provide large matrix for THz imaging. Moreover cost of these technologies is not compatible with industrial system applications described in the previous introduction.

From this table it is straightforward that **antenna coupled microbolometers operating at room temperature** is a technology able to fulfill price constraint to deliver THz system for mass market application. Raytheon in the US started research on this topic since 2002 supported by homeland security effort and they displayed already significant results. In fact, at the SPIE Defense & Security conference in Orlando in 2005, they presented a 22x28 THz focal plane with a CMOS reading circuit (SPIE vol.5778). The performances of this device were presented in a qualitative manner only and there was no discussion of the electro-optical performances of the component in terms of sensitivity or equivalent thermal resolution.

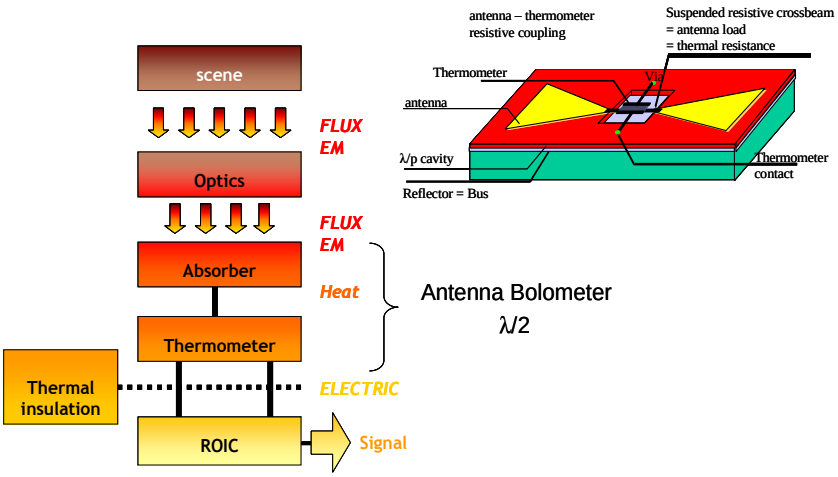

Figure 23. Operating principle of the antenna-coupled microbolometer Existing THz technologies

If we compare it with the European approach, based mainly on **direct detection**, the following technical limitations exist in addition to high

delivery cost. Direct detection includes signal reception on an antenna and its amplification in the same (large) bandwidth, by means of several HEMT (High Electronic Mobility Transistor) stages using GaAs or InP devices. These needs contributed to the development of integration, hybridization and, finally, the appearance of specific integrated circuits: MMICs. These decrease losses by coupling and provide miniaturization, suggesting that integration into a focal plane will be possible. Also, it should be noted that this technology is limited in terms of frequency (spectroscopy for explosives, above 1THz, is not feasible) and currently the cost of the technological lines will not allow mass production.

New terahertz image sensors concepts still need to be found. These should need to match image quality, production cost, power consumption and volume production.

A possible technology for terahertz detection is based on CMOS compatible processing leading to sensors operating at room temperature and capable of low cost production. THz detector principle is slightly different to the IR microbolometer technology due to the fact that absorber and thermometer are physically separated. Metallic antenna enforced with quarter wavelength cavity will provide the coupling with the electromagnetic wave, producing a current flowing into a matched load resistance. Then the thermometer material will sense like a calorimeter the heat coming from THz radiation Joule effect on the load. Schematic presentation of the operating principle is displayed on the picture below

5 OUTLOOK: THE FUTURE OF SEMICONDUCTOR IMAGE SENSING

Thanks to the amazing, relentless progress of semiconductor technology, in particular the specialized CIS processes which are derived from mainstream CMOS processes, we will soon have more cameras than people on earth. This fact has a rather simple consequence, namely that many more pictures will be acquired than can be looked at by human beings, which is particularly true and worrying in the case of security and surveillance cameras. For this reason, experts agree on the direction electronic imaging will progressively take in the future: Image sensors need to be equipped with an ever-increasing amount of digital processing power, enabling these imagers not only to acquire pictures but also to improve the pictures' quality with suitable post-processing and to extract meaningful information about the contents of a scene using powerful object recognition and classification

hardware. The goal will be single-chip machine vision systems that “understand” what they see.

Impressed by the demonstration of image sensors with more and more integrated functionality, a prominent researcher in the field proclaimed the imminence of such "seeing chips", already two decades ago [12]. It is true that for certain tasks, a few examples of image sensors with complete, integrated image processing hardware have been reported, such as single-chip fingerprint recognition and identification systems. Other types of smart image sensors have been demonstrated that are capable of carrying out a few important, but still only rather basic functions for the vision process on a single chip. The more research results are reported, however, the more obvious it becomes that "vision is difficult", as suspected in [12]. It is clear now that early expectations of monolithically integrated single-chip vision systems were too high. While it is possible today to co-integrate an image sensor and all the necessary processing circuitry on a single chip for the solution of a given, not too complex machine vision problem, such an accomplishment is far removed, though, from the original idea of a seeing chip, capable of visually perceiving important aspects of an imaged scene.

The main obstacle is not a technological one; today, a lot of digital processing power and memory can be packed onto a single chip. The problem is rather our still very limited understanding of the natural vision process and how to translate it into reliably working algorithms, for which dedicated circuitry can be fabricated on a “smart” image sensor. Despite almost 50 years of research in machine vision, the man-made, robust machine vision system performing as well as natural vision systems, such as the visual sense of insects, is still elusive. Recent research is increasingly taking clues from the successful natural vision systems, where evidence can be found that all kinds of cognitive functions in humans are implemented with the same basic functionality and system architecture, the so-called “Mountcastle observation” [13]. This is an exciting prospect, of course, that may not only lead the way to “seeing chips” but also to “hearing microphones” and – more generally – to “aware sensors”. In any case, all these developments clearly require more insight and for its implementation more microelectronic functionality on each chip – more Moore, and more than Moore!

6 REFERENCES

[1] S. M. Sze, "Semiconductor Devices — Physics and Technology", 2nd edition, John Wiley & Sons, Inc., New York, 1992.

[2] T. Spirig, "Smart CCD/CMOS Based Image Sensors with Programmable, Real-time, Temporal and Spatial Convolution Capabilities for Applications in Machine Vision and Optical Metrology", Thesis work, ETH Zurich, No. 11993, 1997, chapter 3.

[3] P.J.W. Noble, "Self-Scanned Silicon Image Detector Array", *IEEE Trans. El. Dev.*, Vol. 15, pp. 202-209, 1968.

[4] E.R. Fossum, "Active Pixel Sensors: Are CCD's Dinosaurs?", *Proc. SPIE*, Vol. 1900, pp. 2-14, 1993.

[5] H.S. Wong, "Technology and Device Scaling Considerations for CMOS Imagers", *IEEE Trans. El. Dev.*, Vol. 43, pp. 2131-2142, 1996.

[6] G. Agranov et al., "Super Small, Sub 2µm Pixels For Novel CMOS Image Sensors", *Proc. 2007 Internat. Image Sensor Workshop*, pp. 307-310, 2007.

[7] P. Seitz, "Solid-State Image Sensing", in *Computer Vision and Applications — A Guide for Students and Practitioners*, B. Jähne and H. Haussecker (Eds.), pp. 111-152, Academic Press, San Diego, 2000.

[8] Y.Lim et al., "Stratified Photodiode – A New Concept for Small Size High Performance CMOS Image Sensor Pixels.", *Proc. 2007 Internat. Image Sensor Workshop*, pp. 311-315, 2007

[9] N. Wyrsch et al. "Vertical integration of hydrogenated amorphous silicon devices on CMOS circuits", *Mater. Res. Soc. Symp. Proc.*, Vol. 869, pp. D1.1.1-D1.1.12, 2005.

[10] P. Seitz, "Smart Pixel Arrays", in *Encyclopaedia of Modern Optics*, B. Guenther and D. Steel (Eds.), Elsevier, Oxford, 2005.

[11] A. Krimsky, N. Khaliullin and H. Rhodes, "A 2 e^- Noise 1.3 Megapixel CMOS Sensor", *Proc. 2003 IEEE Workshop on Charge-Coupled Devices and Advanced Image Sensors*, May 15-17, 2003

[12] C. Koch, "Seeing Chips: Analog VLSI Circuits for Computer Vision", *Neural Computation*, Vol. 1, pp. 184-200, 1989.

[13] J. Hawkins, and S. Blakeslee, "On Intelligence", Henry Holt and Company, Inc., New York, 2004.

[14] Steve Tanner, Stefan C. Lauxtermann, Martin Waeny, M. Willemin, Nicolas Blanc, Joachim Grupp, Rudolf Dinger, Elko Doering, Michael Ansorge, Peter Seitz, and Fausto Pellandini," Low-power digital image sensor for still-picture image acquisition", Proc. SPIE Int. Soc. Opt. Eng. 4306, 358 (2001)

[15] K.B. Cho, A Krymski, E.R: Fossum, "A Micropower Self-Clocked Camera-on-a-Chip", IEEE Workshop on Charge-Coupled Devices and Advanced Image sensors, pp. 12-13, June 7-9, 2001 Cal-Neva Resort, Nevada USA; K.B. Cho et al, "A 1.2V

Micropower CMOS Active Pixel Image Sensor for Portable Applications", ISSCC Digest of Tech. Papers, pp. 114-115, Feb. 2000.

[16] www.weinbergervision.com; www.photron.com; www.aostechnologies.com; www.visionresearch.com; www.redlake.com; www.pco.de; www.dalsa.com;

[17] Etoh T.G. & al., "An image sensor which captures 100 consecutive frames at 1000000 fps", IEEE trans. on Electron Devices, Vol.50 No.1, pp.144-151, January 2003

[18] Kleinfelder S. & al., "A 10kframe/s 0.18 um CMOS digital pixel sensor with pixel-level memory", proc. IEEE ISSCC-01 conf., vol. XLIV, pp. 88 - 89, February 2001

[19] S. Lauxtermann, P. & al., "A high speed CMOS imager acquiring 5000 frames/sec", dig. IEDM '99 conf, pp.875-878, December 1999

[20] Zhou Z, Pain B., Fossum E.R., "CMOS active pixel sensor with on-chip successive approximation analog-to-digital converter", IEEE trans on Electron Devices, Vol.44 No.10 pp.1759-1763, October 1997

[21] Krymski A. & al. "A High Speed, 500 fps, 1024 x 1024 CMOS Active Pixel Sensor", IEEE VLSI Circuits conf. Dig, pp.137-138, June 1999

[22] Micron Technology Inc. "MT9M413 1.3 Mpix CMOS Active Pixel Digital Sensor", Datasheet, Ver. 3.0, Jan-.2004

[23] Yadid-Pecht O. & al., "A random access photodiode array for intelligent image capture", IEEE trans on Electron Devices, Vol.38 No.8 pp.1772-1780, August 1991

[24] Krymski A., Tu N., "A 9VLux-s 5000fps 512 x 512 CMOS Sensor", IEEE trans on Electron Devices, Vol.50 No.1 pp.136-143, January 2003

[25] Kleinfeld S. "High-speed, high-sensitivity, low-noise CMOS scientific image sensors", proc. SPIE, Vol 5274, pp.194-205, March 2004

[26] Inoue T & al., "A CMOS Active Pixel Image Sensor with In-pixel CDS for High-Speed Cameras", proc. SPIE, Vol 5580, pp.293-300, 2005

[27] Aerts R. & al., "1.4Gpix/s, 2.9Mpix CMOS image sensor for readout of holographic data memory", proc. IEEE international Image Sensor Workshop, Ses.06 pp.74-77, June2007

[28] Furuta M. & al., "A High-Speed, High-Sensitivity Digital CMOS Image Sensor with a Global Shutter and 12-bit Column-Parallel Cyclic A/D Converters", IEEE JSSC, Vol. 42 No. 4 pp.766-774, April 2007.

[29] Takayagani I. & al., "A 600x600 Pixel, 500fps CMOS Image Sensor with 4.4um Pinned Photodiode 5-Transistor Global Shutter Pixel", proc. IEEE international Image Sensor Workshop, Ses.17 pp.287-290, June2007

[30] Nitta Y. & al., "High-Speed Digital Double Sampling with Analog CDS on Column Parallel ADC Architecture for Low-Noise APS", proc. IEEE ISSCC'06, pp.2024-2031, 6-9 Feb 2006

[31] Krymski A., "A High Speed 4 Megapixel Digital CMOS", proc. IEEE international Image Sensor Workshop, Ses.06 pp.78-81, June2007

[32] Cools T. & al., "An SXGA CMOS image sensor with 8Gbps LVDS serial link", proc. IEEE international Image Sensor Workshop, Ses.17 pp.283-286, June2007

[33] Krymski A., Tajima K. “CMOS Image Sensor with integrated 4Gbs Camera Link Transmitter”, proc. IEEE ISSCC'06, pp.2040-2049, 6-9 Feb 2006

[34] Kawahito S. “CMOS Imaging Devices for New Markets of Vision Systems”, IEICE trans. on Electronics, Vol E90-C No10 pp.1858-68, Oct-2007

[35] Johansson R. & al., “A Multi-Resolution 100 GOPS 4 Gpixels/s Programmable CMOS Image Sensor for Machine Vision“, proc IEEE workshop on CCD & AIS, May 2003

[36] T. Oggier et al., “An all-solid-state optical range camera for 3d real-time imaging with sub-centimeter depth resolution (swissranger),” Proc. SPIE 5249, pp. 534–545, 2003.

[37] R. Lange and P. Seitz, “A solid state time-of-flight range camera,” IEEE Journal of Quantum Electronics 37, p. 390, 2001.

[38] R. Kaufmann et al., “A time-of-flight line sensor - development and application,” Proc. SPIE 5459, pp. 192–199, 2004.

[39] www.mesa-imaging.ch, www.canesta.com, www.pmdtec.com

[40] www.mesa-imaging.ch/prodviews.php

[41] I.A.H. Izhal, T. Ushinaga, T. Sawada, M. Homma, Y. Maeda, and S. Kawahito, “A CMOS time-of-flight range image sensor with gates on field oxide structure,” Proc. 4th IEEE Int. Conf. Sensors, pp.141– 144, Nov. 2005.

Chapter “X ray imaging References”

[1] B. Braun, Electromedica 70 (2002) 1.

[2] J.P. Moy, Thin Solid Films 337 (1999) 213.

[3] A. Oppelt (Ed.), Imaging Systems for Medical Diagnosis, Publicis Corporate Publishing, Erlangen, 2005.

[4] L.D. Hubbard, R.J. Brothers, W.N. King, L.X. Clegg, R. Klein, L.S. Cooper, A.R. Sharrett, M.D. Davis, J. Cai, Ophthalmology 106 (1999) 2269.

[5] M. Hoheisel, L. Ba¨ tz, Thin Solid Films 383 (2001) 132.

[6] M. Hoheisel, J. Giersch, P. Bernhardt, Nucl. Instr. and Meth. 5ANS-531/1–2 (2004) 75.

[7] M. Hoheisel, L. Ba¨ tz, T. Mertelmeier, J. Giersch, A. Korn, Modulation transfer function of a selenium-based digital mammography system, in: IEEE Proceedings of the Nuclear Science Symposium, Medical Imaging Conference, 2004, pp. 3589–3593.

[8] S. Thunberg, H. Sklebitz, B. Ekdahl, L. Ba¨ tz, A. Lundin, H. Mo¨ ller, F. Fleischmann, G. Kreider, T. Weidner, Proc. of SPIE 3659 (1999) 150.

[9] R.A. Street, W.S. Wong, S. Ready, R. Lujan, A.C. Arias, M.L. Chabinyc, A. Salleo, R. Apte, L.E. Antonuk, Proc. of SPIE Med. Imaging Conf. 5745 (2005) 7.

[10] G.B. Avinash, K.N. Jabri, R. Uppaluri, A. Rader, F. Fischbach, J. Ricke, U. Teichgra¨ ber, Proc. of SPIE 4684 (2002) 1048.

[11] J.M. Lewin, P.K. Isaacs, V. Vance, F.J. Larke, Radiology 229 (2003) 261.

[12] L. Tlustos, R. Ballabriga, M. Campbell, E. Heijne, K. Kincade, X.

Llopart, P. Stejskal, Imaging properties of the Medipix-2 system exploiting single and dual energy thresholds, in: Proceedings of the IEEE Medical Imaging Conference, Rome 2004, N43-3, 2004.
[13] M. Hoheisel, R. Lawaczeck, H. Pietsch, V. Arkadiev, Proc. of SPIE 5745 (2005) 1087.
[14] E. Pisano, et al., Radiology 214 (2000) 895.
[15] S.W. Wilkins, T.E. Gureyev, D. Gao, A. Pogany, A.W. Stevenson, Nature 384 (1996) 335.

[Chapter “infrared image sensors”]

[1]« Electrical Doping of HgCdTe by Ion Implantation and Heat Treatment », G. Destefanis; Communication (invited): 3rd International Conference on II-VI Compounds. Monterey (USA) july 1987; Publication: J.Crystal Growth 86(1988) pp.700-727
[2]« HgCdTe Infrared Diodes Arrays », G. Destefanis; Communication (invited): Nato Workshop on Narrow Bandgap Semiconductors; Oslo (Norway) 1991; Publication: Semicond. Sci. Technol. 6 (1991) pp88-92
[3]« Large Improvement in HgCdTe Photovoltaic Detector Performance at LETI », G. Destefanis, J.P. Chamonal; Communication: The US workshop on the Physics and Chemistry of II-VI Materials. Danvers (USA) october 1992 ; Publication : Journal of Electron. Mater.vol 22 n°8 1993 pp.1027-1032
[4]« High performance LWIR 256 x 256 HgCdTe Focal Plane Array Operating at 88 K », G. Destefanis, P. Audebert, E. Mottin, P. Rambaud ; Communication: Interantional SPIE Conference Orlando (USA) april 1997 ;Publication: Proceeding SPIE vol 3061 pp. 111–116 (1997)
[5]« SOFRADIR approach for 2/5 and 3rd generations of IR detectors » P. Tribolet, P. Bensussan, G. Destefanis; Communication: The 5th International Military Sensing Symposium : 2002DTB04 – dec 2002 Wahington (USA) - Org. OTAN. Publication: to be published in the meeting proceedings
[6]« Recent developments of high complexity HgCdTe focal plane arrays at LETI infrared laboratory » G. Destefanis, A. Bain, J. Baylet, P. Castelein, E. De Borniol, O. Gravrand, F. Marion, A. Million, Ph. Rambaud, F. Rothan, J.L. Martin, P. Martin,; Communication The 2002 Workshop on the physics of II VI material, nov 2002, San Diego, USA; Publication : J.Electron mater vol 32 n°7
[7]« Progress in MCT large staring arrays» F.P. Pistone, S.Dugalleix, P.Tribolet, G.Destefanis, – Communication : International SPIE meeting Infrared detectors and focal plane arrays VIII: (San Diego USA august 2006). Publication SPIE proceedings (vol 6295-21)
[8]« HgCdTe large staring arrays at Sofradir » P.Tribolet, G.Destefanis – Communication: The 19th International technology conference on photoelectronis and nigh vision devices (2006) – Publication: to be published in SPIE proceedings
[9]« MWIR focal plane arrays made with HgCdTe grown by MBE on germanium substrates » P. Tribolet, S..Blondel, P.Costa, A.Combette, L. Vial, G. Destefanis, Ph. Ballet, J.P. Zanatta, , O. Gravrand, C. Largeron, JP. Chamonal, A. Million – Communication : International SPIE meeting Infrared technology and application XXXII: (Orlando USA April 2006). Publication SPIE proceedings (vol 6206-82)
[10]« MBE HgCdTe growth on Ge for the 3rd generation of infrared detectors » J.P. Zanatta, G. Badano, Ph. Ballet, J. Baylet, O. Gravrand, J. Rothman, P. Castelein, JP. Chamonal A. Million, G. Destefanis – Communication: The 2005 US Workshop on the Physics and

Chemistry of II VI materials (Boston USA, sept 2005) – Publication: J.Electron.Mater. 2006 vol 35, 6

[11]« TV/4 dual band HgCdTe infrared focal plane arrays with a pitch of 25µm and spatial coherence» J. Baylet , Ph. Ballet, P. Castelein, F. Rothan, M. Fendler, E. Laffosse, JP. Zanatta, JP. Chamonal, A. Million, G. Destefanis – Communication: The 2005 US Workshop on the Physics and Chemistry of II VI materials (Boston USA, sept 2005) – Publication: J.Electron.Mater. 2006 vol 35, 6

[12]« From visible to infrared: a new approach » P.Chorier, P.Tribolet, G.Destefanis, – Communication: International SPIE meeting Infrared technology and application XXXII: (Orlando USA April 2006). Publication SPIE proceedings (vol 6206-01)

[13]« From LWIR to VLWIR FPAs made with HgCdTe at Defir » O.Gravrand, E. Deborniol, G.Destefanis, A.Manissadjian, P.Tribolet, C.Pautet, P.Chorier – Communication : International SPIE meeting Sensors, Systems and Next generation SatellitesXII (Stockholm Sweden September 2006). Publication SPIE proceedings (vol 6361-42)

[14]« From LWIR to VLWIR FPAs made with HgCdTe n+n/p ion implantation technology » O. Gravrand, E. Deborniol, G. Destefanis – Communication: The 2006 US Workshop on the Physics and Chemistry of II VI materials (Newport USA, oct 2006) – Publication: to be published J.Electron.Mater. 2007

[15]«Characterization of high performances long wave and very long wave HgCdTe staring arrays» E. Deborniol, G. Destefanis, A. Manissadjian, P. Tribolet– Communication : International SPIE meeting : Remote sensing (Bruges Belgium sept 2005). SPIE proceedings (vol 5978-44)

[16]«Long wave HgCdTe staring arrays at Sofradir: from 9µm to 13+µm cut-off for high performance applications» A. Manissadjian, P. Tribolet, G. Destefanis, E. Deborniol – Communication: International SPIE meeting Infrared technology and application XXXI: (Orlando USA April 2005). Publication SPIE proceedings (vol 5783)

[17]« Status of HgCdTe bicolour and dual band infrared focal plane arrays at LETI » G.Destefanis, J.Baylet, P.Ballet, F.Rothan, O.Gravrand, J.Rothman, J.P.Chamonal, A.Million – Communication (Invited): The 2006 US Workshop on the Physics and Chemistry of II VI materials (Newport USA, oct 2006) – Publication: to be published J.Electron.Mater. 2007

[18]« Bi-color and dual band infrared focal plane arrays at Defir » G.Destefanis, Ph. Ballet, J.Baylet, P.Castelein, O.Gravrand, J.Rothman, F.Rothan, G.Perrais, J.Chamonal, A.Million, P.Tribolet, B.Terrier, E.Sanson, P.Costa, L.Vial – Communication (Invited): International SPIE meeting Infrared technology and application XXXII: (Orlando USA April 2006). Publication SPIE proceedings (vol 6206-27)

[19]«Demonstration of a 25µm pitch dual band HgCdTe infrared focal plane array with spatial coherence» P. Ballet, P. Castelein, J. Baylet, E. Laffosse, M. Fendler, F. Pottier, S. Gout, C. Vergnaud, S. Ballerand, O. Gravrand, JC. Desplanches, S. Martin, JP. Zanatta, JP. Chamonal, A. Million, G. Destefanis – Communication: International SPIE meeting Optics and Optoelectronics: (Bruges Belgium sept 2005). Publication: SPIE proceedings (vol 5978-44)

[20]«Third generation and multicolour IRFPA developments: a unique approach based on Defir» P. Tribolet, G. Destefanis – Communication (invited): International SPIE meeting Infrared technology and application XXXI: (Orlando USA April 2005). Publication SPIE proceedings (vol 5783)

[21]F. Ma, et al. Phys. Rev. Lett., 95, 176604 (2005)

[22]R. Alabedra, et al., IEEE Trans. Electron Devices, ED-32, 1302 (1985) ; G. Levêque et al., Semicond. Sci. Technol. 8 1317 (1993)

[23]J.D. Beck, C.-F.Wan, M.A. Kinch, J.E. Robinson, Proc. SPIE, 4454, 188 (2001); J.D. Beck, C.-F. Wan, M.A. Kinch, J.E. Robinson, P. Mitra, R. Scrithfield, F. Ma, J. Campbell, J. Electron. Mater. 35, 1166 (2006)

[24]« Gain and Dark current characteristics of planar HgCdTe avalanche photodiodes » G.Perrais, O. Gravrand, J.Baylet, G. Destefanis and J.Rothman– Communication: The 2006 US Workshop on the Physics and Chemistry of II VI materials (Newport USA, oct 2006) – Publication: to be published J.Electron.Mater. 2007

[25]« Gain and Dark current characteristics of planar HgCdTe avalanche photodiodes » G.Perrais, O. Gravrand, J.Baylet, G. Destefanis and J.Rothman– Communication: The 2006 US Workshop on the Physics and Chemistry of II VI materials (Newport USA, oct 2006) – Publication: to be published J.Electron.Mater. 2007

[26]« Demonstration of multifunction bicolour avalanche gain in HgCdTe FPA » G.Perrais; J.Rothman, G.Destefanis, J.P.Baylet, P.Castelein, J.Chamonal; P.Tribolet – Communication : International SPIE meeting Electro optical and infrared systems: technology and applications III (Stockholm Sweden September 2006). Publication SPIE proceedings (vol 6395-16)